MICROSCOPIC FUEL CONSUMPTION MODELLING FOR HAULAGE TRUCKS USING DISCRETE-EVENT SIMULATION

A THESIS SUBMITTED TO
THE GRADUATE SCHOOL OF NATURAL AND APPLIED SCIENCES
OF
MIDDLE EAST TECHNICAL UNIVERSITY

BY

ELİF KINA

IN PARTIAL FULFILLMENT OF THE REQUIREMENTS
FOR
THE DEGREE OF MASTER OF SCIENCE
IN
MINING ENGINEERING

FEBRUARY 2021

Approval of the thesis:

MICROSCOPIC FUEL CONSUMPTION MODELLING FOR HAULAGE TRUCKS USING DISCRETE-EVENT SIMULATION

submitted by **ELİF KINA** in partial fulfillment of the requirements for the degree of **Master of Science** i**n Mining Engineering, Middle East Technical University** by,

Prof. Dr. Halil Kalıpçılar
Dean, Graduate School of **Natural and Applied Sciences** ________________

Prof. Dr. N. Emre Altun
Head of the Department, **Mining Engineering** ________________

Assist. Prof. Dr. Onur Gölbaşı
Supervisor, **Mining Engineering, METU** ________________

Examining Committee Members:

Prof. Dr. Bahtiyar Ünver
Mining Engineering, Hacettepe University ________________

Assist. Prof. Dr. Onur Gölbaşı
Mining Engineering, METU ________________

Assist. Prof. Dr. Ahmet Güneş Yardımcı
Mining Engineering, METU ________________

Date: 15.02.2021

I hereby declare that all information in this document has been obtained and presented in accordance with academic rules and ethical conduct. I also declare that, as required by these rules and conduct, I have fully cited and referenced all material and results that are not original to this work.

Name Last name : Elif Kına

Signature :

ABSTRACT

MICROSCOPIC FUEL CONSUMPTION MODELLING FOR HAULAGE TRUCKS USING DISCRETE-EVENT SIMULATION

Kına, Elif
Master of Science, Mining Engineering
Supervisor: Assist. Prof. Dr. Onur Gölbaşı

February 2021, 104 pages

Mining is one of the machine-intensive sectors, and a vast amount of energy is consumed in many stages of mining operations. Among these operations, haulage systems hold a significant share in energy consumption. At this point, diesel fuel, a form of fossil fuel, is frequently used for haul trucks such that fuel-induced cost becomes a major contributor to the operating cost, especially in surface mining. Fuel consumption also leads to greenhouse gas emissions, in addition to its financial burden. Therefore, monitoring and evaluating fuel consumption rates become an essential topic for mining companies to keep the economic and environmental parameters under control. Various models, classified under macroscopic, mesoscopic, and microscopic approaches, have been used in the literature to characterize vehicle fuel consumption behaviors. Macroscopic and mesoscopic models generally analyze large traffic zones by using a regression-based average speed approach. On the other hand, microscopic models can estimate the instantaneous fuel consumption and emission rates, considering dynamic vehicle speed changes and interactions between vehicles and the ground.

On this basis, the current research study aims to develop a discrete event simulation (DES) algorithm for evaluating fuel consumption and emission rates of haul trucks by using a microscopic modeling approach. The parameters related to vehicle, road, operation, environment, and weather were included in the model. The developed model was applied for a cement company using real operational and environmental datasets. The company has one processing plant and two limestone and clay mines, located 16 km and 7.6 km away from the processing plant. The material haulage operation from the mines to the processing plant is performed using twenty-nine trucks, and each one has a payload capacity of around 40 tonnes. It was observed that fifteen different routes with different operational intentions are available in the area. The model enables dynamic decisions on which routes should be activated for which truck in a real-time line. In this sense, monitoring and recording the fuel consumption and carbon emission rates of both individual trucks and the fleet are achieved in the model. The results show that the average fuel consumption values are 0.51 L/km and 0.46 L/km for the loaded and empty travels between the limestone mine and the crusher in the processing plant. On the other hand, loaded and empty travel values from the clay mine to the plant are observed to be 0.72 L/km and 0.42 L/km.

Keywords: Fuel Consumption, Microscopic Fuel Consumption Models, Mining Trucks, Discrete Event Simulation

ÖZ

AYRIK OLAY SİMÜLASYONU İLE NAKLİYE KAMYONLARI İÇİN BİR MİKROSKOBİK YAKIT TÜKETİM MODELİ GELİŞTİRİLMESİ

Kına, Elif
Yüksek Lisans, Maden Mühendisliği
Tez Yöneticisi: Dr. Öğr. Üyesi Onur Gölbaşı

Şubat 2021, 104 sayfa

Madencilik sektörü, makine yoğun sektörlerden biridir ve madenlerde gerçekleştirilen operasyonların birçok aşamasında fazla miktarda enerji tüketilmektedir. Bu operasyonlar arasında nakliye, enerji tüketiminde önemli bir paya sahiptir. Bir tür fosil yakıt olan dizel yakıt, nakliye operasyonlarında kamyonlar için enerji kaynağı olarak kullanılmaktadır. Kamyonlar çok fazla miktarda yakıt tüketirler ve yakıt maliyeti, yerüstü madenciliğindeki işletme maliyetler içerisinde büyük bir yer kaplamaktadır. Ayrıca, yakıt tüketimi, sera gazı emisyonları gibi bazı çevresel sorunlara neden olabilmektedir. Bu yüzden, yakıt tüketiminin izlenmesi, finansal ve çevresel açıdan maden şirketleri için önemli bir konudur. Makroskobik, mezoskobik ve mikroskobik modelleme yaklaşımlarını içeren modeller, yakıt tüketimi hesaplamaları için literatürde kullanılmaktadır. Makroskobik ve mezoskobik modeller, regresyon bazlı ortalama hızları kullanarak, genellikle yoğun trafik bölgelerinin analizinde kullanılırlar Mikroskobik modeller ise kamyon hızına bağlı olarak değişen anlık yüketim ve emisyon oranlarını tahmin etmek için kullanılırlar.

Bu yapılan çalışma, mikroskobik modelleme yaklaşımını kullanarak anlık olarak tüketilen yakıt miktarını ve emisyon oranlarının tahmini için bir ayrık olay simülasyon modeli geliştirmeyi amaçlamaktadır. Tüketilen yakıt miktarı belirlenirken kamyonlar, yol koşulları ve çevre ile ilgili bazı parametreler ele alınmıştır. Geliştirilen model, bir çimento şirketinden alınan gerçek operasyonel ve çevresel veriler kullanılarak uygulanmıştır. Şirket, içinde kırıcıların olduğu bir işletme tesisi ve bu tesise sırasıyla 16 km ve 7.6 km uzaklıkta bulunan kalker ve kil madenleri bulunmaktadır. Nakliye operasyonları için yirmi dokuz adet 40 ton kapasiteli kamyonlar kullanılmaktadır. Madenler ve işletme tesisi arasında gidilebilecek on beş farklı rota bulunmaktadır. Model, gelen kamyonun hangi rotada ilerleyeceğini dinamik olarak karar vermektedir. Bu nedenle modelde, hem her kamyon için hem de filo için tüketilen yakıt miktarı ve emisyon oranı bulunabilmektedir. Bu sonuçlara göre, sırasıyla dolu ve boş kamyonlar için kalker madeni ve kırıcı arasında gidilen mesafe başına ortalama yakıt tüketimi 0.51 L/km ve 0.46 L/km'dir. Kil madeni ile kırıcı arasında ise dolu kamyonlar gidilen mesafe başına ortalama 0.72 L/km, boş kamyonlar ise 0.42 L/km yakıt tüketirler.

Anahtar Kelimeler: Yakıt Tüketimi, Mikroskobik Yakıt Tüketim Modelleri, Maden Kamyonalrı, Ayrık Olay Simülasyonu

To My Family

ACKNOWLEDGMENTS

First of all, I would like to express my sincere gratitude to my supervisor Asst. Prof. Dr. Onur Gölbaşı for his endless help, guidance and patience during this long journey. His support and understanding helped me to overcome every struggle that I had faced since the beginning of my master's degree. It was a great opportunity to be supervised by him. I would also like to thank examining committee members, Prof. Dr. Bahtiyar Ünver and Asst. Prof. Dr. Ahmet Güneş Yardımcı for accepting to be a part of the committee and for their valuable comments and suggestions.

I would like to thank all my friends, especially Merve Karagözoğlu and Simin İşleyici for supporting and motivating me during my study. In addition, I would also like to thank Sena Şenses and Furkan Şahiner for their help, suggestions and comments. Moreover, I would like to express my special thanks to Taha Serbest who went through all stages of my thesis study with me with his endless support, patience and everlasting belief in me.

And finally, I am deeply indebted to my dear family, Feray Kına, Fuat Kına and Zeynep Kına for their endless and unconditional love, support and encouragement in my whole life. I could not be here without you.

TABLE OF CONTENTS

LIST OF TABLES

TABLES

LIST OF FIGURES

FIGURES

CHAPTER 1

INTRODUCTION

1.1 Background

In recent years, energy-related financial and environmental considerations have become more than an issue that should be settled domestically and globally. Intensive energy usage, especially in machine-dominant production industries, needs to be evaluated holistically to control greenhouse gas emissions and seek opportunities to decrease the share of energy consumption per unit of production. Mining is one of the machine-intensive sectors where economic extraction of minerals should be managed using various machinery with high production rates to provide the manufacturing sector's raw material requirement. Operability of mining and processing activities in a mine site requires massive energy usage such that 12 percent of the overall energy consumption in industries is occupied only by mining activities (EIA, 2019).

Areas of energy utilization in a mining area may vary depending on the operations, classified in exploration, extraction, haulage or hoisting, and processing. Electricity and diesel fuel are the most common energy consumed in mines, where about 32 percent of the total energy is only used in haulage operations (Bajany *et al.*, 2017). Haulage refers to a process of conveying ore or waste material to the prespecified destinations in a mining site. Truck and excavator dispatching systems are the most common way of haulage operations in surface mines. In those activities, a remarkable amount of fuel is consumed by trucks, and it becomes a major contributor to operating cost and carbon emissions.

Surface mining production, different from other industries, requires haulage of a massive amount of materials in a demanding working environment where the fuel cost, depending on the configuration of the truck fleet, may account for 60% of the total operating cost with the highest share (Rodovalho *et al.*, 2016). Therefore, any operational improvement in a haulage system is expected to provide a noticeable energy-saving and operating cost reduction. Another issue arising from intensive fuel consumption is greenhouse gas emissions at a substantial rate, leading to an environmental sustainability problem. Trucks emit a considerable amount of pollutants by burning fuel, which are carbon dioxide (CO_2), carbon monoxide (CO), hydrocarbons (HC), nitrogen oxides (NO_x). In particular, CO_2 plays a leading role in the greenhouse effect. Greenhouse gas emissions increase proportionally concerning the amount of fuel consumed. As a result, reducing energy consumption can help to pull down the mining-induced greenhouse gas emissions.

There are various factors effective in the fuel consumption rate of trucks. Therefore, single or multiple of these factors should be evaluated to create energy-saving opportunities in a mining operation area. These factors need to be analyzed so that trucks' mutual and dynamic interactions that variate fuel consumption behaviors should be adequately modeled. On this basis, fuel consumption and carbon emission models can be classified as macroscopic, mesoscopic, and microscopic models depending on their scales of parameters. This research study utilizes a microscopic modeling approach to detail and analyzes individual and multiple vehicles' fuel consumption profiles in a joint operation. Accordingly, sub-models of force, motion, and fuel consumption are constructed in a discrete-event environment, and the developed algorithm is applied for a real case study in mining.

1.2 Problem Statement

In surface mining, trucks are commonly used in material haulage operations. Diesel fuel, a type of fossil fuel, is used in trucks as an energy source. Since many trucks need to be employed in these operations, the total fuel consumption leads to a remarkable financial burden for companies. Besides, greenhouse gas emissions as a waste product of fuel burning in engines can create an environmental issue around the mining area. Therefore, any improvement in energy-saving policies related to trucks may help have noticeable cost reductions and more sustainable operations for mining companies. The characterization of fuel consumption behavior is complex and requires an interactional evaluation of the mining environment, fleet configuration, production schedule, and road network specifications. Therefore, triggering and effective factors in determining the fuel rate profiles of active trucks in an operable mine need to be discussed using micro-level kinematic variations to draw representative conclusions.

1.3 Objectives and Scopes of the Study

This research study aims to develop a discrete event simulation (DES) model to evaluate trucks' performance in terms of their fuel consumption rates by using microscopic modeling. Sub-objectives of the research can be listed as follows:

i. Developing and correlating sub-modules in a DES environment related to the force, motion, and fuel consumption estimation

ii. Determining the kinematic variables such as acceleration and speed profiles of individual trucks for each road segment with different road characteristics

iii. Estimating greenhouse gas emissions related to the fuel-burning rate

iv. Implementing the algorithm for a cement company using actual operational and environmental datasets

Under the research scope, haul trucks with a payload capacity of 40 tonnes are analyses in the model implementation. These trucks are used for a cement production activity where two mines and one processing plant are included in the operation area with a travel networking holding multiple routes.

1.4 Research Methodology

This research study uses both deterministic and stochastic approaches to reveal the truck fuel consumption behavior in a mine haulage system. Figure 1.1 represents an overview of the research methodology steps. These methodology steps are discussed as follows:

i. Determination of Effective Parameters: Identifying technical and operational parameters that affect trucks' fuel consumption rates in compliance with the related literature.

ii. The DES model development: The DES model at the microscopic level is developed considering the micro-scale kinematic interactions between the operational environment and vehicles. Accordingly, force, motion, and fuel sub-modules are developed, considering various stochastic and deterministic factors. For any road network holding multiple routes of different activity intentions and a truck fleet specification, the algorithm may provide second-, segment-, and road-level fuel performance of individual trucks and fleet itself.

iii. Acquisition and Processing of Application Data: Technical and operational datasets are obtained from a cement company and vehicle catalogs.

iv. Implementation of the DES Model: The developed model is applied for the input dataset of a cement operation with continuous and real-time monitoring of fuel performance indicators in the DES environment of Arena Software.

v. Evaluation and Analysis of Results: Fuel consumption of individual trucks and the whole operating fleet are estimated in a real-time environment with locational interactions. Besides, greenhouse gas emissions are also simulated as an output of fuel consumption. The results are discussed and compared for each road segment with different road characteristics.

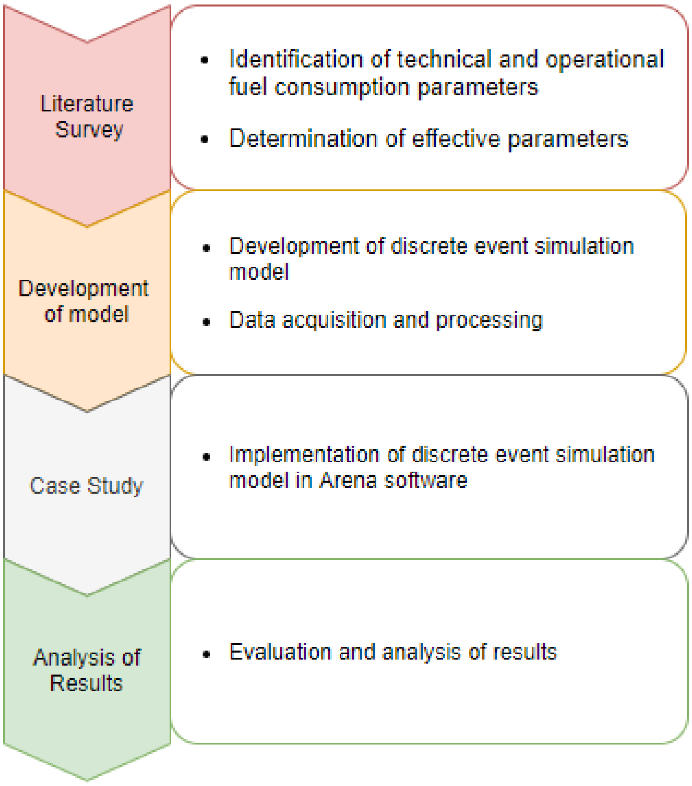

Figure 1.1. Research Methodology Steps of the Research Study

1.5 Expected Contributions of This Thesis

In the literature, various studies have been performed about fuel consumption estimation using different solution approaches to evaluate the vehicle fuel-burning process's financial and environmental aspects. In many machine-intensive industries, especially in mining, machines consume a high amount of fuel per unit production. This situation leads to a tremendous operating cost and greenhouse gas emission. Therefore, improving fuel consumption rates in production industries can make noticeable differences in operations' profitability and environmental effects. The simulation model constructed in the current study can reveal instantaneous haul truck fuel consumption and carbon emission behaviors regarding different road, vehicle, and weather conditions. In this way, mining companies may forecast and evaluate their fuel-induced parameters to achieve a fuel-saving solution.

CHAPTER 2

LITERATURE REVIEW

This chapter presents a literature review on fuel consumption and carbon emission studies. First, to better understand the thesis topic, some background information on fuel consumption and the resultant emission problems are provided. Then, the leading factors of fuel consumption and emission rates are discussed. After that, different fuel consumption models, which are also used in the estimation of fuel emission rates, are mentioned in detail. This chapter is concluded with fuel consumption studies in mining haulage systems.

2.1 Background Information about Fuel Consumption and Emissions

Transportation is an essential requirement for economic development and improvement of human welfare as it provides access to resources. As countries' economies grow, the importance of the transportation sector increases worldwide and is expected to increase in the coming years. However, although transportation has positive effects on socio-economic systems, it also has negative consequences such as congestion caused by the increase in vehicles and the traveling times (Walsh, 2003). These consequences lead to an increment in demand and energy usage for transport systems, so the transportation sector has a significant role in total energy consumption. Vehicles generally consume fossil fuel as an energy source, and diesel oil, a form of fossil fuel, is used in road transportation. Some amount of different pollutants are emitted simultaneously due to fuel burning in engines. An increasing rate of energy consumption, and emissions of pollutants like carbon dioxide, pose a severe problem for human health and the environment. Especially, harmful greenhouse gas emissions can cause global warming that may result in climate change. For this reason, reducing both energy consumption and emission rates worldwide have become a priority in the state- and sector-based regulations.

In the world, five main sectors have a significant role in energy consumption (Figure 2.1). The industrial sector involves facilities, construction, and mining. The transportation sector includes transportation by car, truck, aircraft, ship, and train. The residential sector covers accommodation areas. The last one is the commercial sector that contains offices, hospitals, schools, and malls. As seen in Figure 2.1, the transportation sector is one of the most energy-intensive sectors. In the year 2018, according to data from the U.S. Energy Information Administration (EIA), 28% of the total energy consumption in the U.S. is occupied by the transportation sector. Transporting by road, air, rail, and maritime are the transportation modes, and road transportation has the highest share among them by a percentile weight of 85%. Different energy sources such as petroleum, biofuels, natural gas, and electricity are used in transportation systems, and petroleum usage is comparatively dominant as the primary energy source (EIA, 2019; Rodrigue, 2020).

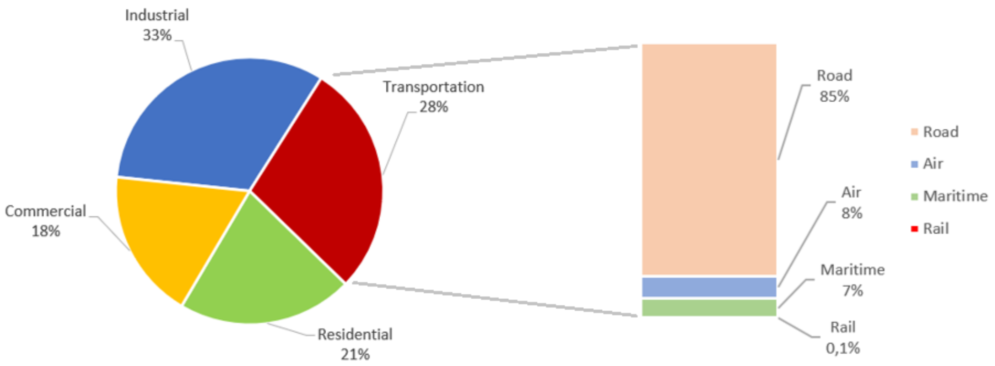

Figure 2.1. Share of the Total Energy Consumption in the U.S.

Transportation plays a significant role in pollutant emissions since petroleum is still dominant in transportation systems. On this basis, vehicles emit a considerable amount of different pollutants such as carbon dioxide (CO_2), carbon monoxide (CO), hydrocarbons (HC), nitrogen oxides (NO_x), and particulate matter (PM). Among these pollutants, the main research focus is given to CO_2 since it is predominantly emitted from vehicles and may lead to critical environmental issues. In this sense, a particular term named carbon footprint refers to the total amount of emissions, especially CO_2 (Morse, 2018).

In Figure 2.2, the pie charts represent the total CO2 emissions' percentile weights according to the sectors, transportation types, and vehicles utilized in road transport, respectively. According to the European Union (2015) data, the transportation sector accounts for 32% of the total CO_2 emission, where road transport is responsible for 75% of the total CO_2 emission of the transportation sector. It is clear from Figure 2.2 that the contributing factors of transportation have a significant influence on the global CO_2 emission, and any improvement in the fuel consumption efficiency will provide positive control over the carbon emission rates.

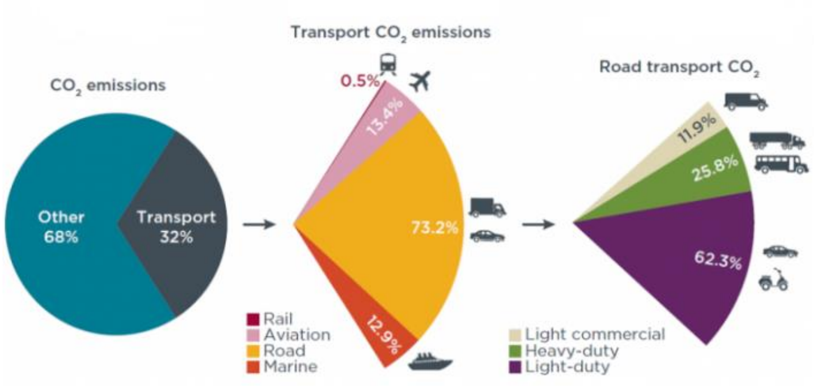

Figure 2.2. Distribution of Carbon Dioxide Emissions in the European Union in 2015 (Hockenos and Wehrmann, 2018)

Emitted pollutants have serious adverse effects on the environment and are categorized into three groups as direct, indirect, and cumulative effects. At this point, CO emissions and noise are considered under the direct effects. On the other hand, indirect effects have higher harmful effects than direct effects. Particulates from incomplete combustion like CO_2 and NO_x are examples of these effects and threaten human health with respiratory and cardiovascular problems. Lastly, cumulative effects are the combinational forms of both direct and indirect effects. Global warming and climate change are classified under the cumulative impact (Rodrigue, 2020). In this sense, greenhouse gases trap the sun's heat, and this process is named the greenhouse effect. An increase in greenhouse gas and pollutant emissions above limits is the main reason for climate change leading to global warming.

Many countries worldwide intend to minimize greenhouse gas emissions and energy consumptions by embedding the related rules into their regulations so as to recover the adverse effects of energy consumption on the environment. As explained previously, the transportation sector is one of the major contributors to pollutant emissions, and any improvement in the emission rates will have a noticeable impact. In this aspect, research that focuses on energy consumption efficiency and vehicle emissions reduction has become one of the literature's prioritized topics. On this basis, the main factors effective on fuel consumption and the resultant gas emissions are discussed in Section 2.2 for a holistic evaluation of the problem.

2.2 Factors Affecting Fuel Consumption

Various parameters can affect the fuel consumption and emission rates of vehicles. Ahn and Rakha (2002) and Zhou et al. (2016) suggested that these parameters can be classified into six categories: travel, weather, vehicle, roadway, traffic, and driver. The main variables of each category can be seen in Figure 2.3. In the following sections, each category will be explained in detail.

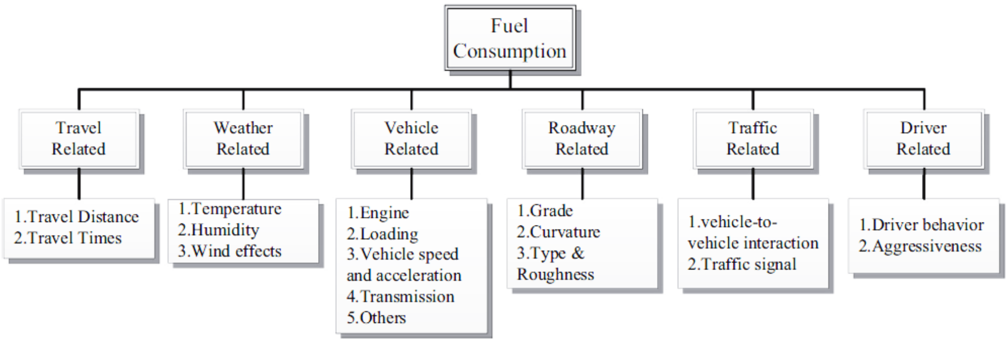

Figure 2.3. Factors that Affecting Fuel Consumption (Zhou *et al.*, 2016)

2.2.1 Travel Related Factors

The main contributing factors under this category are travel distance and travel times. Generally, drivers tend to choose the routes with the shortest travel distance or the fastest travel time. However, according to a study by Ericsson *et al.* (2006), these routes do not always ensure the least fuel consumption or emission rates. Very short distance trips generally exhibit a higher fuel consumption than long-distance trips. The main reason is that the vehicle engine cannot reach its operating temperature during a short trip, which is also named as cold start effect. Cold start occurs at the initial stages of the trip, and the fuel consumption rate starts to decrease once the working components and the engine of the vehicle get warmer. Moreover, at the initial phases of vehicle movement, vehicles tend to emit more greenhouse gas. Therefore, a long-distance trip may lower fuel consumption than short-distance trips (Zacharof *et al.*, 2016).

There are various studies that intend to build up a correlation between route alternatives and fuel consumption rates. The shortest or fastest route is not always the best alternative because of road properties or traffic conditions from the perspective of fuel consumption and emissions. Ahn and Rakha (2008) investigated the effect of route choice on fuel rate. Their results showed that approximately 20% of fuel could be saved by selecting an alternative route that is even 5 minutes longer but with better road and traffic conditions. Boriboonsomsin *et al.* (2012) demonstrated that the optimal route for fuel consumption and emission, defined as an eco-friendly route, can be different from the shortest or fastest route. According to their results, nearly 13% fuel saving can be provided by 16% longer route. Masikos *et al.* (2015) also achieved fuel and energy savings of approximately 21% by choosing an energy-efficient route that is 1.45% longer in the distance as an average and 10.26% longer in travel time than other routes.

2.2.2 Weather Related Factors

Weather-related factors are temperature, humidity, and wind effects. These factors can have both direct and indirect impacts on fuel consumption and emissions. It is hard to control and measure the weather-related factors in real-time. So, they are accepted as the least effective among the other factors in terms of controllability (Zhou *et al.*, 2016). Fuel consumption is expected to increase at low ambient temperatures because air density becomes denser in winter and cold days compare to the warmer days, and it causes a higher aerodynamic resistance. Oppositely, on warm days with high ambient temperature, aerodynamic resistance decreases, and fuel consumption also decreases accordingly. Besides, vehicles' working components easily reach their efficient operating temperatures in warmer climates, reducing fuel consumption and emissions (Fontaras *et al.*, 2017). These conditions can be assumed to happen due to the direct effect of temperature. The use of vehicle accessories like air conditioners can be assumed to be an indirect effect of ambient temperature. On this basis, Pekula *et al.* (2003) focused on the effect of ambient temperature on heavy-duty trucks. The study results showed that fuel consumption and emission rates were higher at the higher ambient temperatures because of the frequent air conditioning system usage.

Most of the related literature studies have focused on temperature but not weather conditions such as rain and snow. Yao *et al.* (2020) classified the weather conditions in detail and discussed them from environmental and safety perspectives. At this point, fuel consumption increases under rainy and snowy weather conditions. These conditions change the properties of the road surface and so the rolling resistance. Vehicle tires' handling ability decreases on rainy and snowy surfaces, and tires can exhibit redundant rotations due to slippage that causes an increment in fuel consumption.

Humidity and wind conditions, which concern the speed and the wind direction, affect air resistance. Air resistance and humidity are inversely proportional. Air resistance decrease when humidity increases since dry air is denser than humid air.

For this reason, fuel consumption also decreases. A wind velocity of 3 m/s can increase or decrease air resistance according to wind direction up to 10%, so fuel consumption can be affected by air resistance (Ligterink *et al*., 2016).

2.2.3 Vehicle Related Factors

Vehicle-related factors associated with the engine, vehicle shape, loading, vehicle speed, acceleration, transmission, accessories, and operating age are the major contributors to fuel consumption and the resultant emissions. Engine size that variates according to the vehicle type directly determines the fuel consumption performance. On this basis, U.S. Environment Protection Agency (EPA,2016) categorizes vehicles into three main groups as light-duty, medium-duty, and heavy-duty vehicles according to their weights. Light-duty vehicles have smaller engine capacities, and their fuel consumption rate is expected to be less than the vehicles of the other groups. Operating a large-capacity vehicle instead of two small-sized vehicles can help reduce fuel consumption in total (Demir *et al.*, 2014).

Vehicles using power-driven accessories such as air conditioner has a higher fuel consumption rate. Besides, transmission type in a vehicle affects the fuel consumption rate. Due to technological improvements, new-generation vehicles with automatic transmission have a lower fuel consumption rate nowadays, while automatic transmissions led to more fuel usage than manual transmission in the past (EPA, 2019).

Vehicle weight is another important factor for fuel consumption. When the vehicle weight increases, more operating power is required, so fuel consumption starts to accelerate. This condition also causes a greater amount of carbon emission in proportion to the fuel burned (Feng *et al.*, 2005). Various studies investigate the effect of vehicle weight on fuel consumption. According to Mickünaitis *et al.* (2007), an increment in vehicle weight by 100 kg may cause a fuel consumption growth by 6.5% for petrol engines and 7.1% for diesel engines. Plotkin and Ribeiro (2009) also investigated the correlation between the reduction rates in vehicle weight and fuel consumption. The research results show that a 10% weight reduction can achieve approximately 6% of fuel saving.

Speed and acceleration are the most important elements of the fuel consumption variation since they directly impact the vehicle movement's required power. Parreira and Meech (2011) and Demir *et al.* (2012) aimed to find out the optimum vehicle speeds in their studies in such a way that fuel consumption could be minimized under certain constraints. The optimum vehicle speed changes according to different road and traffic conditions. As mentioned above, vehicles are classified into three main categories, which are light-duty (LD), medium-duty (MD), and heavy-duty (HD) according to their weights. In Figure 2.4, Demir *et al.* (2011) compared the speed levels of these vehicle types in terms of fuel consumption by using a microscopic model explained in the following sections. This graph shows that fuel consumption rates are high at low-speed levels regardless of the vehicle type due to fuel usage inefficiencies. Then, fuel consumption rates follow a decreasing trend up to a point where the consumption rate reaches its minimum value at the optimum speed. At higher speed levels, vehicles consume more fuel due to higher aerodynamic resistance. Aerodynamic resistance increases drastically in driving faster since it is proportioned to the square of speed (Plotkin and Ribeiro, 2009). Besides, heavy-duty vehicles have a higher fuel consumption rate for similar speed levels than the other vehicle types since more driving energy is required due to their higher weights. The graph also shows the relationship between emissions and speed, and higher speed levels are observed to induce greater emission rates.

Driving with abrupt acceleration and deceleration is defined as aggressive driving, leading to higher fuel consumption and emissions. Minimizing abrupt acceleration and braking with smooth driving is one solution for reducing fuel consumption and its resultant carbon emission. This concept is related to driver behavior, and drivers need to drive smoothly by realizing the traffic signals and flow to save fuel (Huang *et al.*, 2018). Bigazzi and Bertini (2009) mentioned that keeping aggressive driving under control can reduce emissions by 25%. Aggressive driving and its motivating factors will be discussed in detail in Chapter 2.2.6.

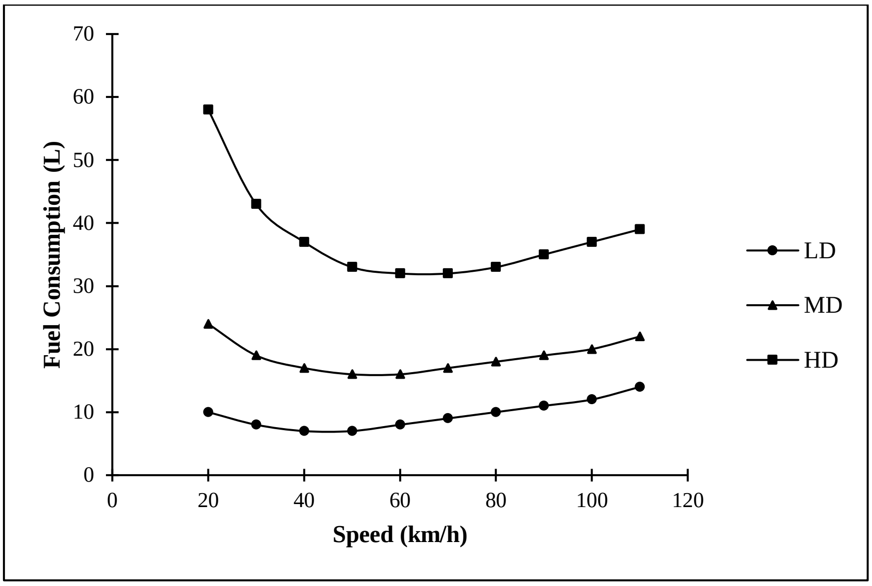

Figure 2.4. Fuel Consumption for Vehicle Types (Demir *et al.,* 2011)

2.2.4 Roadway Related Factors

Roadway related factors refer to physical road characteristics such as grade, texture, and road surface roughness. They are crucial in estimating fuel consumption since power requirements for the same vehicle types show a remarkable variation depending on the road's grade and rolling resistance. Since most power-operated components in a vehicle are related to its design parameters, there is limited access to their power utilization factors. However, a vehicle's response to different road characteristics can be used more effectively in selecting the optimal route if there are multiple alternative routes between the destination points. On this basis, the power requirement is much higher in steeper roads to overcome the gravitational force in an opposite movement, and it causes greater fuel consumption and emissions. Therefore, drivers should avoid choosing routes with steeper road grades (Demir *et al.*, 2014).

Road grade is the most dominant factor among the other road characteristics and may cause drastic fuel consumption changes. The influence of road grade on fuel consumption and emissions was studied in detail by Park and Rakha (2006), Boriboonsomsin and Barth (2009), and Gallus *et al.* (2017). Park and Rakha (2006) aimed to reveal road grades' effect on vehicle fuel consumption and emission rates by comparing three different traffic scenarios. It was concluded in the study that each 1% increment in the road grade may increase the fuel consumption and CO_2 emission rates by 9% approximately. Boriboonsomsin and Barth (2009) evaluated the impact of road grade on fuel consumption and light-duty vehicle emissions using microscopic modeling based on a real dataset. The results showed that a route including a near-flat road profile achieves a fuel-saving between 15% and 20% compared to a rough route covering uphill and downhill road profiles. This saving range was stated to differ for different types of vehicles. Gallus *et al.* (2017) investigate the impact of road grade on emission rates for different road types using the Portable Emission Measurement System (PEMS). The study showed that a change in road grade from 0% to 5% raise CO_2 emissions by 65-81%, depending on the road type.

On the other hand, rolling resistance is the resistive force of the road surface opposite the vehicle motion. The roughness and texture of the road affect the rolling resistance and the resultant fuel consumption. Roughness is defined as the vertical deviations in the road surface, and it is measured by International Roughness Index (IRI). This index can take a value up to 16 mm/m. Lower IRI values refer to goodness in road surface quality, while the highest values stand for the eroded surfaces (Fontaras *et al.*, 2017). Figure 2.5 shows the IRI values for different types of roads. When the roughness of the road surface increases, fuel consumption shows an ascending trend accordingly (Green *et al.*, 2013).

The texture is defined as the planar surface deviation in a road surface, and it also affects the friction resistance by providing a positive contribution to the brake-ability of vehicles. The effect of texture is determined according to wavelength sizes. Higher wavelength leads to higher rolling resistance and increasing fuel consumption.

Changes in the surface texture can help to reduce fuel consumption by 5% to 10% (EAPA, 2004).

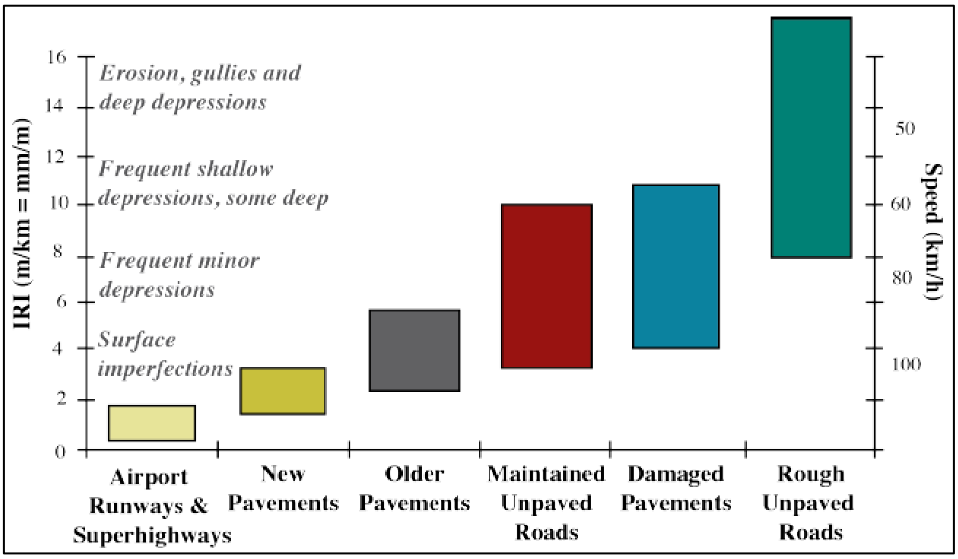

Figure 2.5. IRI Values and Maximum Speeds of Different Types of Roads (Green *et al.*, 2013)

2.2.5 Traffic Related Factors

The movement of vehicles in definite directions under certain rules and obligations are defined as traffic. Traffic-related factors should be considered by including the vehicle and driver's aspects when determining the fuel consumption. Because traffic-related factors such as traffic signaling and congestion affect fuel consumption and emission rates by also influencing the driver behaviors so that it may induce a mutual interaction resulting in decision changes on speed, acceleration, and deceleration (Greenwood, 2003). On this basis, Intelligent Transportation Systems (ITS) are used as advanced communication and information technologies for the transportation systems so as to minimize traffic problems and improve safety. Traffic signal control is one of the ITS strategies to reduce fuel consumption and CO_2 emissions by avoiding rapid accelerations and decelerations at the intersection points or traffic lights and providing a fuel saving up to 47%. There are several studies about the utilization of traffic signal control systems. Asadi and Vahidi (2010) proposed Predictive Cruise Control (PCC) using the upcoming traffic signal information to reduce both idling times at the traffic lights and fuel consumption. According to the timing signal from an upcoming traffic light and safe braking distance, optimal velocities of vehicles are calculated. Their results show that the fuel consumption can be decreased by nearly 47%, where CO_2 emissions can be reduced by 56% with the help of traffic signal information. According to a study by Iwata *et al.* (2012), CO_2 can be reduced by 7% using the Deceleration Support System that is designed to help driver to brake earlier at traffic lights. The research study of Tielert *et al.* (2010) differs from the other studies in terms of the simulation scenarios scale. They introduced the traffic light information to the vehicle communication system to conduct large scale simulation scenarios. The results showed that a fuel-saving up to 22% could be achieved by using these interconnected systems. The study also revealed that CO and NOx emissions could be decreased with a reduction up to 80% and 35%, respectively.

Due to the rapid increase in vehicles, traffic congestion has become a severe problem, especially in urban areas. Congestion is defined as a situation where the traffic movement is restricted due to overmuch vehicle intensity on the same route. It significantly affects fuel consumption and emissions by interrupting the regular vehicle speeds and extending the travel times. Besides, vehicles' idling conditions, which is described as the time while a vehicle engine is running but not moving, are frequently observed in traffic congestion. Any extension in idling time affects fuel consumption efficiency since a vehicle can consume fuel with a rate between 0.6 and 5.7 L/h in an idling condition (Huang *et al.*, 2018). Since fuel consumption efficiency is expressed as distance traveled per fuel volume, the weight of idling time in a total travel time considerably affects the overall efficiency.

For this reason, increasing traffic congestion leads to a remarkable jump in both redundant fuel consumption and emissions. In this sense, fuel consumption can rise to 40% but averagely 26% in congested traffic conditions than the same route without any congestion (De Vlieger *et al.*, 2000; Zacharof *et al.*, 2016). Barth and

Boriboonsomsin (2008) investigated the impact of traffic congestion on emissions. The results proved that emission rates could be decreased by 7% to 12% with the improved traffic operations reducing congestion levels.

New technologies can also help to decrease the adverse effects of idling conditions. The start-stop system is an example of these new technologies and automatically switches off the vehicle's engine in an idling state. At this point, Fonseca *et al.* (2011) investigated the effect of the start-stop system, and it is shown that more than a 20% decrease in CO_2 reduction can be achieved compared to a vehicle without any start-stop system. Bigazzi and Clifton (2015) modeled the effects of congestion on fuel consumption for different vehicle characteristics. It is revealed that an increasing level of congestion leads to higher fuel consumption rates when the average vehicle speed is low. On this basis, fuel consumption has the highest rate if vehicles move with an average speed under 20 mph at high congestion levels.

2.2.6 Driver Related Factors

Driver related factors concern driving behavior and driver aggressiveness levels correlated with speed and acceleration profiles of vehicles. Drivers can exhibit their own driving characteristics that may induce a variation in speed, acceleration, deceleration, and gear shifting profiles of vehicles. These profiles may cause remarkable differences in fuel consumption rates even for similar type vehicles. Individual factors such as age, gender, psychology, experience in driving, traffic culture, and personal characteristics can trigger driving behavior. Brundell-Freij and Ericsson (2005) indicated that driver age has a significant effect on average speed such that drivers having age over 60 tend to drive at slower average speeds. Another study by Khader and Martin (2019) showed that emission rates vary for different age groups and genders. The study defends that the young female driver group displays lower emission rates at the same route. Moreover, inexperienced drivers were detected to consume more fuel than experienced drivers due to abrupt acceleration and braking behaviors (Zhou *et al.*, 2016; Khader and Martin, 2019).

Aggressive driving and eco-driving concepts are directly related to driving behavior. Aggressive driving can be characterized by the behaviors where over-speed, abrupt acceleration, and abrupt deceleration are experienced so that a greater rate of fuel consumption can be observed compared to a smooth driving style. In contrast to aggressive driving, eco-driving aims proper driving of a vehicle by avoiding over-payload, abrupt acceleration and deceleration, and not using unnecessary accessories to minimize the environmental impact of fuel usage. Changing the driving behavior from aggressive to smooth driving may help to decrease fuel consumption in a range between 20% and 45% (Meseguer *et al*., 2017; Javanmardi *et al.*, 2017; Sivak and Schoettle, 2012).

Many researchers intend to evaluate and discuss driving behaviors by including their effects on fuel consumption rate. On this basis, Meseguer *et al*. (2017) classified drivers into three categories according to driving styles as quiet, normal, and aggressive drivers. Quiet driving is defined as conservative driving by avoiding sudden speed changes. According to the analyses, aggressive driving was detected to cause the highest fuel consumption. On this point, aggressive drivers were observed to consume about 1.2 liters of fuel more per 100 km compared to quiet drivers. It means that any behavior changes from aggression to quite a driver can help achieve a fuel-saving up to 20%.

Similarly, Javanmardi *et al.* (2017) categorized driving behaviors into aggressive driving, eco-driving, and normal driving. These categories have different acceleration, deceleration, and speed patterns. It was revealed from the study that 3.65 liters per 100 km could be saved in a pass from aggressive to eco-driving. Fuel consumption is detected to be 40% more for aggressive driving compared to normal driving due to frequent acceleration and braking attempts. Sivak and Schoettle (2012) identified eco-driving decisions in strategic, tactical, and operational levels that may influence fuel consumption and emissions. Operational decisions involve driving behaviors in speed, acceleration, idling, and the other factors where driver decisions are effective. According to the observations, a fuel saving of 25% can be achieved per driver by implementing eco-driving techniques.

A brief summary of the contributing factors of fuel consumption discussed in Chapter 2 is given in Table 2.1. The following chapter will discuss the quantitative models used in the estimation of fuel consumption.

Table 2.1. *A Summary of Contributing Factors of Fuel Consumption*

Factor	Effect	Reference
Travel	20% fuel saving by route selection	Ahn and Rakha (2008)
	13% fuel saving by choosing an eco-friendly route	Boriboonsomsin *et al.* (2012)
	21% fuel saving by the selection of energy-efficient route	Masikos *et al.* (2015)
Weather	At high temperature, fuel consumption decreases	Fontaras *et al.* (2016)
	At high temperature, fuel consumption increases because using air conditioning	Pekula *et al.* (2003)
	Fuel consumption increases in rainy and snowy weathers	Yao *et al.* (2020)
	Increase in humidity results in to decrease in air density, air resistance, and so fuel consumption decreases 10% fuel saving according to the direction of the wind	Ligterink *et al.* (2016)
Roadway	Fuel consumption increase by 9%, with 1% increase in road grade	Park and Rakha (2005)
	15-20% higher fuel consumption in a hilly route than the flat route	Boriboonsomsin and Barth (2009)
	65-81% higher CO_2 emissions with the change in road grade by 0-5%	Gallus *et al.* (2017)
	When road roughness increase, the fuel consumption increase	Green (2013)
	Fuel-saving by 5-10% with changes in texture	EAPA (2004)

Table 2.1. *A Summary of Contributing Factors of Fuel Consumption (cont'd)*

Factor	**Effect**	**Reference**
Traffic	47% fuel and 56% CO_2 reduction with traffic signal information	Asadi and Vahidi (2010)
	7% CO_2 reduction with using upcoming traffic light signal	Iwata *et al*. (2012)
	22% fuel saving by traffic light information	Tielert *et al*. (2010)
	Up to 40% but averagely 26% increase in fuel consumption at congested traffic conditions	De Vlieger *et al.* (2000) & Zacharof *et al*. (2016)
	7-12% emission reduction with reducing congestion level	Barth and Boriboonsomsin (2008)
	20% CO_2 reduction by start-stop	Fonseca *et al.* (2011)
Driver	Drivers over 60 years consume less fuel	Brundell-Freij and Ericsson (2005)
	Young female drivers produce less CO_2	Khader and Martin (2019)
	Inexperienced drivers consume more fuel than experienced drivers	Zhou *et al.* (2016)
	20% higher fuel consumption in aggressive driving	Meseguer *et al.* (2017)
	Up to 40% higher fuel consumption in aggressive driving	Javanmardi *et al*. (2017)
	25% fuel saving by eco-driving	Sivak and Schoettle (2012)

2.3 Fuel Consumption and Emission Models

This section reviews the vehicle fuel consumption and emission models in detail. As mentioned before, fuel consumption and emission rates are correlated with each other, and CO_2 emission is directly proportional to the amount of fuel consumed. Therefore, fuel consumption models and emission models can be handled and discussed together in a typical structure.

These models are used to estimate and evaluate fuel consumption rates of vehicles and the resultant emissions produced from transportation systems. On this basis, there are various models that differ according to their modeling approaches, structures, and input data. Faris *et al.* (2011) categorized modeling types according to five different aspects:

i. The scale of the input variables,
ii. Formulation approach,
iii. Type of explanatory variable,
iv. State variable value, and
v. The number of dimensions.

The scale of the input variables is the most frequently observed aspect of classifying models in the literature. This modeling aspect has three main subcategories according to their aggregation level of the input variables:

i. Macroscopic models,
ii. Mesoscopic models,
iii. Microscopic models

In macroscopic models, the fuel consumption rate is evaluated according to the average speeds of vehicles. In microscopic models, instantaneous fuel consumption and emission rates are estimated using instantaneous kinematic variables such as speed and acceleration. Mesoscopic models use the scales of input data aspects that are between macroscopic and microscopic scales. In mesoscopic models, fuel consumption rates are calculated for each link. Figure 2.6 represents the categorization of fuel consumption and emission models based on input parameters. According to aggregation levels of the input data, macroscopic models have the highest aggregation level. Oppositely, microscopic models have the lowest aggregation level. The selection of the modeling approach changes depending on the purpose of the study and the detail required.

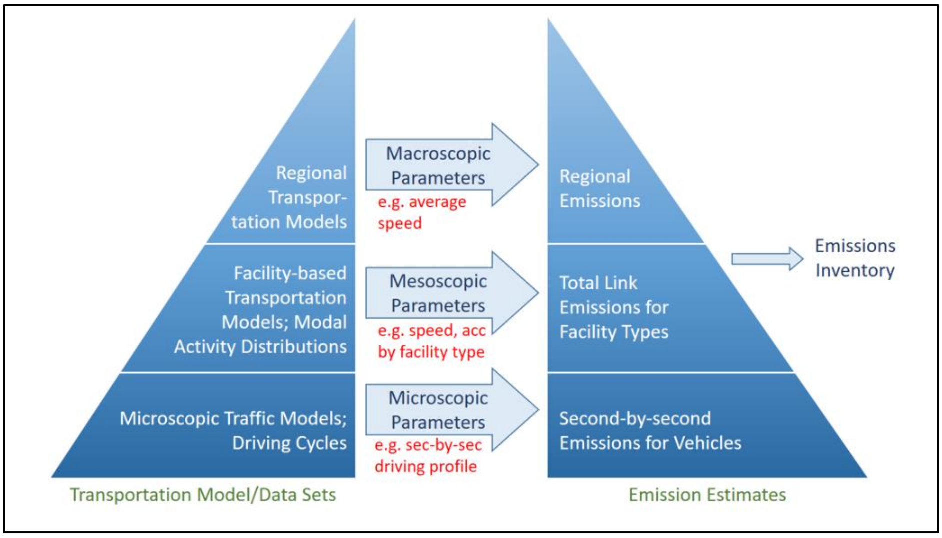

Figure 2.6. Categorization of Fuel Consumption and Emission Models (An *et al*., 1997)

2.3.1 Macroscopic Models

Macroscopic models can also be named regression-based models or static models. These models are used for developing global emission models without detailed information. Macroscopic models are suitable for calculating fuel consumption and emission rates in large-area applications where individual vehicles' consumption details are not much crucial. They use average aggregate network parameters as input data to determine the fuel consumption and emission rates for large scale areas. Network-wide fuel consumption and emission rates are calculated from mathematical equations based on the input parameters such as average speed and total travel distance. The main outputs derived from these models are average fuel consumption and rate in terms of liters per meter and kg per meter, respectively. In macroscopic models, travel-, vehicle-, and weather-related factors are considered. Roadway, traffic, and especially driver-related factors are not used as an input parameter.

Macroscopic models provide average emission factors of each pollutant like CO_2, CO, NO_x for each vehicle type as a function of average speed during a trip. Different average fuel consumption and emission rates can be calculated for each different average speed input. A typical example of the macroscopic model function can be viewed in Figure 2.7. This figure shows the line fitting of an average speed function to estimate the variation of NO_x emission for different average speed values for a specific vehicle type.

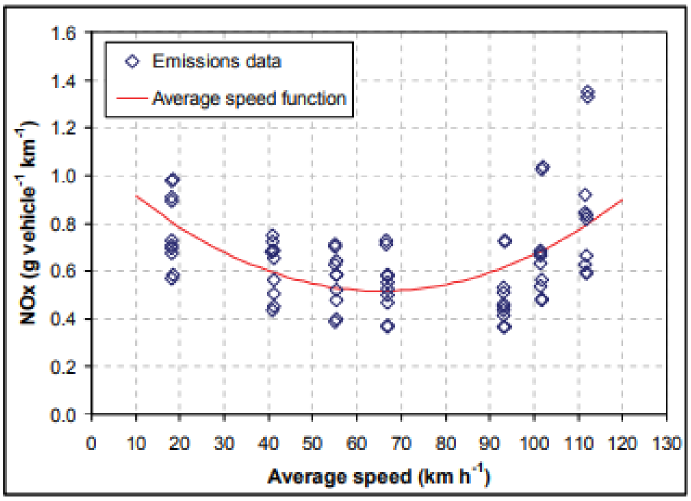

Figure 2.7. Average Speed Function for NO_x (Barlow *et al*., 2001)

These models are frequently used in many studies owing to their advantages. They are relatively easy and practical to use, and less detailed input data are required to construct the models comparatively. On the other hand, some limitations become valid when using these models. As stated previously, the main focus in the macroscopic models is given to determine the average speed and emissions. At this point, the same fuel consumption and emission rates are obtained from the same average speed values regardless of driving styles. However, it should be noted that driving behavior also has a considerable effect on the consumption rate and emissions. This situation can be considered as the fundamental limitation of macroscopic models. It becomes more problematic, especially for lower average speeds due to higher variations in driving behavior. On the other hand, it is less challenging for higher average speeds since the variations in driving styles are more limited (Barlow and Boulter, 2009). Another limitation is that they are advised to be used where the average speed is less than 50 km/h since these models do not reflect an increase in aerodynamic resistance at high speeds (Akcelik, 1985). Although several macroscopic models have been developed in the literature, this chapter will discuss the common models called MEET, COPERT, MOBILE, and EMFAC.

MEET: It was developed under a European Commission's project, and its extension stands for 'Methodologies for Estimating air pollutant Emissions from Transport' model. The model aims to calculate emissions and evaluate the air pollution effect of transportation systems by generating regression functions of average speed function from actual measurements. MEET can be used to estimate emissions and fuel consumptions of not only road transportation but also railways, water and air transportation systems (Barlow and Boulter, 2009).

COPERT: Its abbreviation refers to 'Computer Programme to Calculate Emissions from Road Transportation'. It was financed by European Economic Area (EEA), and its initial version was developed in 1989. Similar to MEET, functions of average speeds are used to calculate vehicle emissions from road transport. These functions are specific to vehicles, which have different weights, and they can also be used for estimating fuel consumption (Demir *et al.*, 2014). For heavy-duty vehicles, it is mentioned that COPERT may achieve a more accurate estimation.

MOBILE: Environment Protection Agency (EPA) developed this model first in 1978, and it has been updated periodically. It is also used for calculating emissions like CO, HC, CO_2, and NO_x by using the vehicle's average speeds-based functions. After the latest update in 2004, the MOBILE model was replaced by MOVES, which is also a EPA model (EPA, 2016).

EMFAC: 'Emission Factor' model was developed by the California Air Resources Board (CARB), which is a macroscale model for estimating emissions. Like all the other macroscopic models, EMFAC also calculates emission rates using the derived functions from average vehicle speeds and real-life measurements (Faris *et al.*, 2011).

2.3.2 Mesoscopic Models

Mesoscopic models can be described as the integrated models of macroscopic and microscopic models. For this reason, mesoscopic models use partial properties and similarities of both types. The applications of mesoscopic models are similar to macroscopic models, so that they are also used for relatively large-scale applications where fuel consumptions of individual vehicles are not critical. Different from the macroscopic model, mesoscopic models may also include driving behavior factors. However, mesoscopic models consider more aggregated vehicle groups' driving behaviors instead of individual driver behaviors for different vehicles.

Mesoscopic models are a link by link basis models and use average aggregate link parameters as an input variable to estimate fuel consumption and emission rates for each link. As mentioned before, the aggregation level of input data of mesoscopic models is in a range between macroscopic and microscopic models. Mesoscopic models are less aggregate than macroscopic models. In other words, mesoscopic models use more factors than macroscopic model (Yue, 2008). All the fuel consumption factors discussed in the previous chapter can be considered as input data but not as detailed as in microscopic models. The average fuel consumption and emission rate for each link are calculated as an output. The total consumed fuel and emissions for the network can be found by cumulative these link values. The network is divided into links according to similar traffic and driving behaviors, and links reflect network characteristics. This property facilitates the calculation of total fuel consumed and the related emissions for the network more accurately.

In recent studies, it has been observed that mesoscopic models have become popular in dealing with large-scale fuel consumption and emission rates. First of all, they give more detailed and accurate results than macroscopic models, and also input data requirement and model complexity are less compared to microscopic models. However, dynamic speed profiles and speed and acceleration variations in small time increments are not modeled in these models.

Well-known examples of mesoscopic models are MOVES, MEASURE, and VT-MESO. The common principle in these models is the prediction of fuel consumption according to operating conditions of a vehicle such as acceleration, deceleration, cruise, and idle. So, they can also be described as event-based models. These modes have different average speeds, and different functions are derived from these speed values. Using the functions, fuel consumption and emission rates are calculated for each operating mode. Cumulative of the individual modes is used to estimate the total fuel and emission values.

MOVES: The latest version of MOBILE model was replaced with ‘Motor Vehicle Emission Simulator’, i.e. MOVES, and became the official emission model of EPA. The modal activity was considered in the model instead of the average speed concept to provide accurate estimations of greenhouse gas emissions from vehicles by reflecting operating processes such as cold start and idling phases. Input data of this model are traveled distance, vehicle type, average speed, and link by link traffic data. The main outputs of the model are greenhouse gas and air toxic (Liu, 2015).

MEASURE: Some researchers conducted in The Georgia Institute of Technology developed a model called ‘The Mobile Emission Assessment System for Urban and Regional Evaluation’, MEASURE. It is a modal emission model and provides a mesoscopic estimation of pollutants such as HC, CO, and NO_x. There are two major modules in this model, which are start and on-road emission modules that include operating modes such as accelerating, decelerating, cruising, and idling. Emission rates are calculated from average speed, road characteristics, and traffic data (Faris *et al*., 2011).

VT-MESO: The VT-Meso was developed at Virginia Tech and is a link by link basis model. Its objective is to compute light duty vehicles' fuel consumption and emission rates for different modes similar to MEASURE’s operating modes. By using the input parameters like average speed, the number of vehicle stops per unit distance, and average stop duration, average fuel consumption and emission rates are predicted for each road segment (Yue and Rakha, 2008).

2.3.3 Microscopic Models

Microscopic models are also called dynamic models or instantaneous models. These models are used to estimate instantaneous vehicle fuel consumption and emission rates using detailed data. For instance, disaggregated and kinematic variables such as speed and acceleration are used as primary input data in microscopic models. These input data can show the impacts of a vehicle's dynamic characteristics on fuel consumption and emissions. As model outputs, instantaneous fuel consumption and emission rates are calculated continuously by considering the effects of individual vehicles' driving behaviors in the network. Driving behaviors like aggressive or normal driving have a significant impact on fuel consumption. Therefore, their fuel consumption rates for the identical speed values cannot be similar.

Microscopic models are capable of reflecting the difference in fuel consumption and emission rates of various driving behaviors. Each vehicle's driving behavior is modeled in the network, and the total amount of fuel consumed is estimated by the integration of these instantaneous rates in terms of liters per second. Microscopic models consider all aforementioned factors, especially vehicle related ones, that have an impact on fuel consumption and emissions, thus, they require more detailed data compared to the other types of models. Figure 2.8 shows a presentative illustration of microscopic models. In brief, second by second speed profiles of vehicle are collected from real world measurements and considering road grade, driver behavior, and similar factors, and instantaneous energy consumption and emission rates can be calculated by microscopic models accordingly.

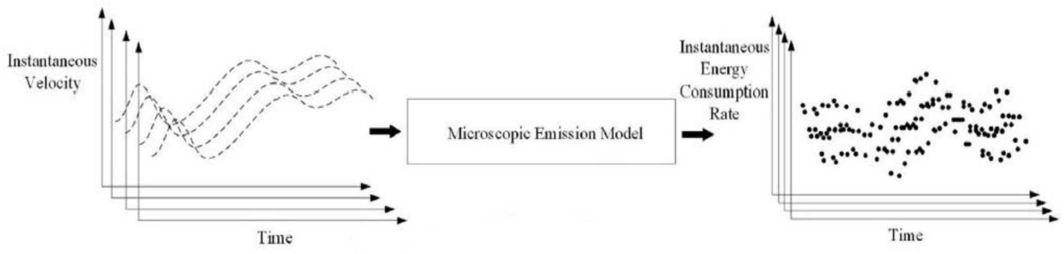

Figure 2.8. Microscopic Modelling Approach (Li *et al*., 2017)

According to their modeling approaches, the microscopic model can be categorized into regression-based models and power (load)-based models. In regression-based models, linear regressions obtained from the relationship between instantaneous speed and acceleration levels are used to calculate fuel consumption and emission rates. Linear regressions represent the relationships between the emissions, speed profiles, and dynamic variables. The best-fit line function can be found and used as a regression-based model among numerous speed and acceleration combinations. However, overfitting may create a problem for these models (Ferrara, 2018). VT-Micro is an example of regression-based microscopic models.

VT-Micro: It was developed by Ahn *et al.* (2002) at Virginia Polytechnic Institute and State University. Different combinations of speed and acceleration levels are taken as input data for obtaining the best-fit line with the lowest uncertainty. Fuel consumption and emission rates are estimated by using the functions of instantaneous speed and acceleration levels of vehicles. The model considers two main different scenarios that concern positive and negative acceleration values. Positive accelerations occur by the generation of increasing engine power in a vehicle while negative accelerations do not require any power generation (Ahn *et al*., 2002).

Power (load)-based models are based on analyzing the physical and chemical processes that cause emissions. They usually have modules that simulate these processes. Essential variables of these models are fuel rate and vehicle-specific power. Fuel consumption and emission rates are calculated by considering engine power, engine speed, and air to fuel ratio. Engine power is the sum of the total tractive power requirements, which is the summation of inertia, rolling and air resistance, and engine power requirements for accessories like air conditioning. Vehicle characteristics, speed, and acceleration levels are important for determining the power requirements. Power-based models require several parameters that are about vehicle characteristics with high complexity. CMEM is one of the most popular models using the microscopic approach.

CMEM: In the late 1990s, 'Comprehensive Modal Emission Model' (CMEM) was developed by researchers at the University of California at Riverside and at the University of Michigan. As referred in the model name, it can estimate fuel consumption and emission rates for a wide range of vehicles under many different conditions. As input data, various vehicle specifications and physical variables are needed to be measured or collected to utilize this model. The model comprises six different modules: power demand, engine speed, air-fuel ratio, fuel rate, engine-out emissions, and catalyst pass fraction. Using these modules, second by second fuel consumption and emission rates of pollutants like CO_2, CO, HC, NO_x can be estimated (Scora and Barth, 2006).

Microscopic models have some advantages over the other types of models. First of all, microscopic models can estimate fuel consumption and emission rates more precisely since they represent many different real-life scenarios by using instantaneous speed and acceleration profiles. Second, microscopic models consider the driving behaviors of a vehicle in the network. As mentioned, in macroscopic models, they assume that each vehicle in the network has shown the same fuel consumption and emission rates regardless of vehicle type and driving behaviors. In addition, microscopic models may be more suitable for local and smaller-scale networks since vehicles' fuel consumption profiles in short time segments need to be performed. Therefore, it may be time-consuming for larger network applications where a homogenous and stable fuel consumption behavior is observed. The comparison of the models is summarized in Table 2.2.

Table 2.2. *A Summary of Contributing Factors of Fuel Consumption*

	Macroscopic	**Mesoscopic**	**Microscopic**
Application Area	Large scale	Medium-scale	Small scale
Main Input	Average aggregate network parameters	Average aggregate link parameters	Instantaneous kinematic variables
Data Requirement	Needs less data	Needs more than macroscopic, less than microscopic	Needs more and specific data
Main Output	Average network fuel consumption and emission rates	Average link fuel consumption and emission rates	Instantaneous fuel consumption and emission rates
Accuracy	Less accurate	More accurate than macroscopic, less accurate than microscopic	More accurate

2.4 Fuel Consumption in Mining Haulage Systems

In mining areas, extracted ore or waste needs to be transported between different destinations such as production face, processing plant, dumpsite, stockpile or any other required locations. Differently from the other industries, a massive amount of materials should be transported in mining with an almost continuous operation, and some specific transportation systems are required in this process. There are two common transportation systems used in mines that are classified under haulage and hoisting. Haulage refers to horizontal transportation generally in surface mining operations where hoisting is used to define vertical transportation in underground mines (Tatiya, 2012). Skip, cage and conveyors are examples of hoisting equipment. On the other hand, trucks, conveyors, and rail systems are used frequently in haulage operations.

A vast amount of energy generated from electrical sources and diesel is consumed predominantly in mining operations such as milling, excavating, and haulage. Figure 2.9 represents the share of energy consumption of various industrial sectors. As seen from the figure, the mining sector is one of the main energy-intensive sectors where about 12% of the total energy is consumed only in mining (EIA, 2019). Since emission rates are correlated with energy consumption, it can be concluded that mining is one of the major contributors to industry-based emissions.

According to Bajany *et al.* (2017), 32% of the total energy used in mines is consumed by transportation operations. Besides, transportation operations account for approximately half of the total operating costs in mining, and fuel cost is the main cost item (Rodovalho *et al.*, 2016). Among these systems, truck haulage is the most common type of transportation in surface mining. They generally use diesel fuel as an energy source. Since payload capacities and gross weights of mining trucks are generally high, which can variate according to truck type, their operating performances have a remarkable effect on mines' fuel consumption amounts. For these reasons, companies and researchers have searched for proper solutions to reduce fuel consumption with financial and environmental concerns. Therefore, any improvement in fuel usage efficiency may contribute to keeping pollutant emissions and operating costs under control in mining.

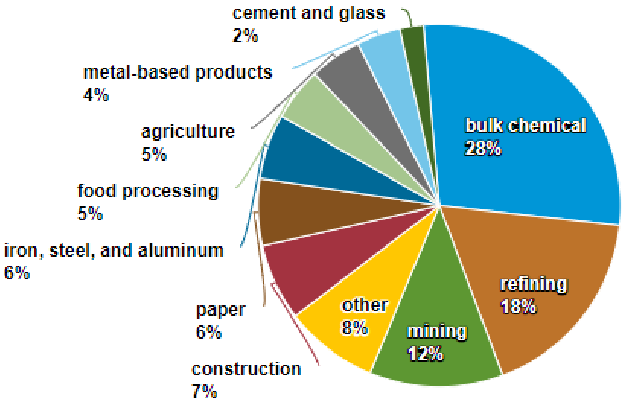

Figure 2.9. Energy Consumption for Different Industry Sectors in U.S. (EIA, 2019)

There are various studies that intend to discuss and evaluate the fuel consumption dynamics of the transportation sector. However, in the literature, a few of them are related to mining haulage systems. This chapter mainly concentrates on the previous studies about fuel consumption behavior of mining trucks since operating environment and vehicle types in mining may differ from the transportation systems in the other areas.

Saboohi and Farzaneh (2009) developed a model to optimize driving strategies based on speed and gear ratio so as to minimize fuel consumption. The study considered not only vehicle parameters but also driver and traffic-related factors. Fuel consumption rates were calculated for different traffic flow intensities, and different speed and gear shifting profiles were obtained for various scenarios. The study's optimized scenarios showed that a potential fuel saving of 1.5 L per 100 km could be achieved.

Tolouei and Titheridge (2009) studied the relationship between fuel economy and safety by considering the effect of vehicle weight. Fuel consumption rates were detected to be highly correlated with vehicle weight and greenhouse gas emissions. In addition, some other analyses were conducted to evaluate the mutual effects of weight and transmission types. It was concluded that weight might have a higher impact on fuel consumption for automatic transmission vehicles compared to manual transmission vehicles.

Kecojevic and Komljenovic (2010) aimed to establish a relationship between fuel consumption, engine power, and load factor using haul truck data obtained from the operating mines. It was mentioned that fuel consumption has a strong correlation with engine power and load factors. Load factor values change according to the truck payloads and road conditions. Poor haul road conditions and an increase in gross weights cause a jump in load factor. Load factor and fuel consumption have a linear relationship, and a high load factor leads to higher fuel consumption. Reduction in load factor can decrease fuel consumption and also CO_2 emissions.

Awuah-Offei *et al*. (2011) discussed energy efficiency variations for truck and shovel dispatching systems by using the discrete event simulation method. In this basis, some alternative strategies were generated for the improvement of energy efficiency. It was detected in the study that haul road design can be optimized in mine so that fuel consumption can be minimized with decreasing cycle times and supporting production rates.

Fu and Bortolin (2012) analyzed off-road haul trucks' fuel consumption behaviors by considering speed levels and gear shifts. Road topography parameters were stated to affect off-road haul trucks' fuel consumption and should be regarded when minimizing fuel rates. In addition, it was revealed in the study that optimal gear shifts may decrease fuel consumption by 4%, even for the same travel route and travel time.

Sahoo *et al.* (2014) presented a model for minimizing fuel consumption of mine haul trucks. It was tried to detect and optimize the variables that may have an impact on fuel consumption. Factors such as payload, speed, and acceleration were used as input data. By constructing various alternative decisions, it was mentioned that a fuel saving of 17% could be achieved. The study also defends that the generated scenarios can be applicable for different mines with changing design parameters.

Siami-Irdemoosa and Dindarloo (2015) evaluated the impact of mining trucks idle time on fuel consumption and operating cost. The study aimed to find out fuel consumption per cycle by using the artificial neural network technique. The results showed that idle time has a significant role in redundant fuel consumption and greenhouse gas emissions, and the strategies to decrease idle time should be a part of fuel consumption models.

Rodovalho *et al*. (2016) discussed the fuel consumption profiles of mining trucks in a large iron mine. Variables related to fuel consumption in haulage operations were identified and ranked according to their priorities using actual datasets. A macroscopic model based on average speeds of vehicles was developed with regression functions. It was claimed in the study that fuel saving in the mine can be improved by 10% with the proper strategies focusing on primary causes of fuel consumption.

CHAPTER 3

DEVELOPMENT OF THE DISPATCHING ALGORITHM

3.1 Introduction

In open-pit mining, truck dispatching systems convey ore or waste between dynamic or static points, indicating the locations of shovels, crushers, dumpsite, or stockpile, by using haul trucks. The numbers and production capacities of trucks and shovels have significant roles when evaluating the key performance indicators of dispatching systems. Using dispatching systems effectively, truck allocation per excavator/loader should be organized so that waiting times of trucks in a queue should be reduced as well as maximizing productivity and minimizing operational cost. Productivity and operating cost are the most crucial performance indicators of ongoing mining operations. In this sense, productivity is measured in the tonnage of material transported per cycle or per unit time; therefore, decreasing cycle time can improve productivity. On the other hand, operational cost covers all the dynamic and production induced measures such that fuel consumption, as mentioned in the previous chapter, is the main contributor of operating cost in mines with truck haulage systems. In this study, a discrete-event simulation model, which aims to reveal dynamic interactions between truck and road to calculate fuel consumption and mine production per period, was developed. Besides, variation in speed levels for each road segment where road conditions can be changeable and the resultant cycle times can also be monitored and estimated in the simulation environment.

This chapter discussed the logic behind the developed dispatching algorithm and its implementation in a discrete event simulation software. The model requires the computation of some sub-models to calculate effective forces during the movement of trucks, generation of dynamic speed profiles, and fuel consumption to overcome net resistive forces for the resultant speed levels. These sub-models are based on some deterministic and stochastic approaches where calculations are time-based, i.e. dynamic, and the decisions in the simulation steps are taken in discrete periods. In other words, the model evaluates the changes in system status at discrete points of the approaching decisions in time, and it has random variables as inputs. The detailed explanation of these sub-models and the algorithm's steps will be discussed through the flowchart in Section 3.2. In section 3.3, the model's implementation into Arena, which is a discrete event simulation software, will be explained. The behaviors of trucks during a cycle of production between pre-specified locations were modeled using Arena modules. A detailed explanation of these modules and the module flowchart will also be given in this section.

3.2 Algorithm Logic

The developed model is based on microscopic modeling, and it considers each truck's behavior in the mine haulage system. Different truck characteristics such as their models, payload capacities, and acceleration and braking abilities are taken as input data in the model's computation. Their speed profiles variated in small time increments are generated with the model to determine the instantaneous fuel consumption rates. The total amount of fuel consumed per period in the whole haulage system is found by estimating and accumulating these instantaneous rates. Network routes between pre-specified destinations are involved. Interactions between trucks in the queue are also considered in the construction of the model. On this basis, Figure 3.1 illustrates the flowchart of the developed algorithm. The steps given in the flowchart can be explained as follows:

- The simulation starts with introducing truck entities into the algorithm. Then, each truck is assigned to a specific excavator in the system, according to tactical production scheduling plans on a daily basis. According to the monthly weather dataset, the weather condition for the analysis period is determined. On this basis, the available weather condition is used to estimate variables related to the road surface.

- Trucks are allowed to travel through the specified routes considering the loading points and the dumping destinations. The routes are divided into segments according to road grades and intersection points. The segment information is taken as input data. All the influential resistive and assistive forces in that segment and the kinematic variables are calculated to reveal the instantaneous acceleration behavior. These variables are used in the motion model to generate speed profiles. A detailed explanation of the motion model will be discussed in the next section. Fuel consumption rates acquired in each road segment of each route is estimated. Each segment transmits its information and the available truck acceleration and speed behaviors to the sequential segment until the route is ended.
- When the route is completed, the simulation validates the truck location once more to evaluate its queue condition and the expected waiting time. It takes its position and waits in the queue for loading if it is at a loading point. Once the loading operation is completed, and the truck is titled as 'loaded'. The loaded truck leaves the loading points and travels to the crusher if the loaded material is ore. Any truck movement is restricted to a specific route to dump the material, and any other destination is not allowed during that route. Speed levels and fuel consumption rates are calculated in the segment- and the route-basis.
- If the truck arrives at the crusher, it takes its position in the crusher queue. After dumping the material, the model checks the refueling requirement. It is assumed that the truck needs a refueling in case that the fuel level in the tank is below 10 percent of its full capacity. In this situation, the truck takes its route to the fuel station location, and the refueling process occurs for a certain time. The threshold level for refueling is adjustable in the algorithm.
- If the algorithm detects that the truck is unloaded at a dumping location without any requirement of refueling, administrative breaks are controlled. If any shift break or shift change is detected, the truck is allowed to travel to

the parking station and waits until the halt is over. After completing the shift break, trucks are transferred to the assigned excavators and continue their production cycle by taking the segment information of the new route.

- As an alternative option, when there is no shift break, the algorithm controls whether daily production is over or not. Supposing that daily production continues, trucks take the segment information once again and keep the operation going. If the operation day is ended, the algorithm checks whether the observation period has been completed. In the case that the observation period has not been completed yet, the trucks are moved to the parking station and wait until the new day begins. On the other hand, if one year has passed since its beginning, the simulation is completed on an annual basis. Simulation outputs can also be evaluated for a more extended period by including different route options and accumulative estimation of varying simulation runs.

Separate but mutually interactive sub-modules for instantaneous force calculation, motion modeling, and fuel consumption estimation are constructed to perform the model. These sub-modules will be discussed in detail in Sections 3.2.1, 3.2.2, and 3.2.3, respectively.

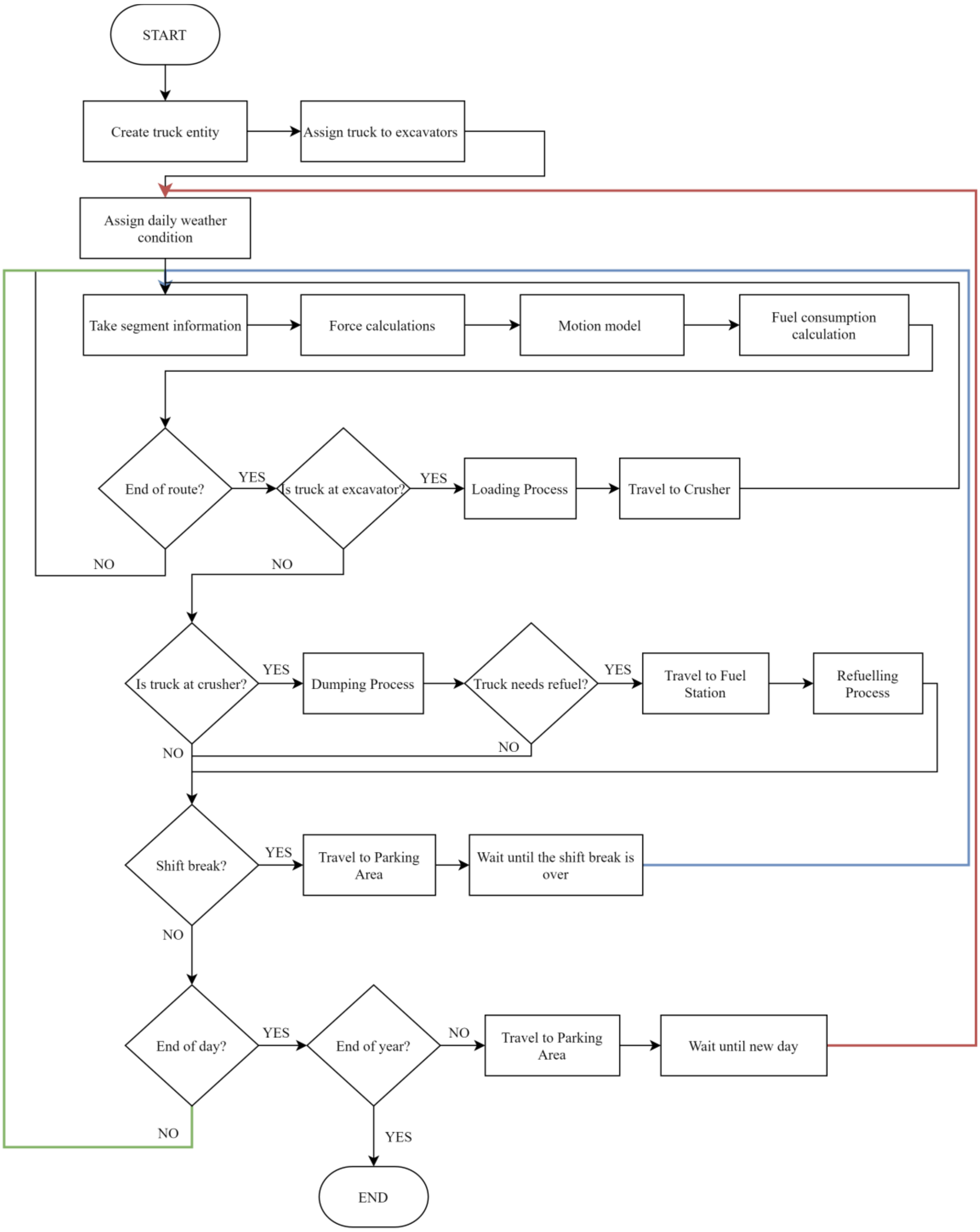

Figure 3.1. The Model Flowchart

3.2.1 Force Calculation Model

In this sub-module, the forces that are effective in the truck movement are calculated by using some fundamental physical dependencies. Figure 3.2 illustrates the truck's body diagram and the acting forces between the truck and the ground. In this sense, there are two main groups of forces considering whether they provide a resistive or assistive contribution on truck movement. Resistive forces include all the forces that have an opposite direction to the truck's motion. In contrast, assistive forces act in the same direction of movement.

Figure 3.2. Body Diagram of Truck (Soofastaei *et al*., 2016)

As shown in Figure 3.2, the acting forces are derived from rolling resistance of ground, road gradient, motor-induced force (rimpull), and drag force of wind resistance. Force caused by rolling resistance (F_{RR}) is always a resistive force no matter truck is moving uphill or downhill direction. Effect of road gradient (F_{GR}) can be either of resistive or assistive forces depending on the gradient in the direction of travel. Rimpull force ($F_{Rimpull}$) is always an assistive force and is rated with the available pushing force induced by the truck motor. In addition, drag force (F_{DR}) applied by the wind on the frontal surface of the truck is always resistive. Therefore, the net force acting on a truck is calculated as given Equations 3.1 and 3.2.

$$F_{net}^{uphill} = F_{Rimpull} - (F_{RR} + F_{DR} + F_{GR}) \tag{3.1}$$

$$F_{net}^{downhill} = (F_{Rimpull} + F_{GR}) - (F_{RR} + F_{DR}) \tag{3.2}$$

3.2.1.1 Rolling Resistance

Rolling resistance is the force that resists the motion of a rolling object over the road surface. In the current case, the rolling objects are the tires of a truck where the gross weight of the truck and load material is active. On this basis, road surface conditions and payload affect the amount of rolling resistance. Equation 3.3 can be used for the calculation of rolling resistance.

$$F_{RR} = 9.81 * W * C_r \tag{3.3}$$

Where:

F_{RR} = Rolling resistance force
W = Total weight
C_r = Rolling resistance coefficient

The rolling resistance coefficient varies according to different types of tires and surfaces since it is related to the interaction between them. Rolling resistance coefficients for various types of road surfaces can be seen in Table 3.1 (Kaufman and Ault, 1977). Weather conditions like snow or rain can influence the road surface properties and so the rolling resistance. The road surface's wetness can increase the rolling resistance coefficient about 20% (Ejsmont *et al.*, 2015).

Table 3.1. *Rolling Resistance for Various Types of Surfaces (Kaufman and Ault, 1977)*

Type of Surface	Rolling Resistance (%)
Cement, asphalt, soil cement	2
Hard-packed gravel, cinders or crushed rock	3
Moderately packed gravel, cinders or crushed rock	5
Unmaintained loose earth	7.5
Loose gravel and muddy rutted material	10 - 20

3.2.1.2 Grade Resistance

Grade resistance is defined as the force due to gravity. It can be either a resistive or assistive force, depending on the movement direction. In the uphill movement, it becomes a resistive force. Oppositely, in the downhill movement, gravity assists the movement, and it is accepted as an assistive force. It is directly affected by the grade of the road, as given in Equation 3.4.

$$F_{GR} = 9.81 * W * G \tag{3.4}$$

Where:

F_{GR} = Grade resistance force
W = Total weight
C_r = Grade of the road (%)

3.2.1.3 Drag Force

Drag force is the force that resists the movement of objects through the surrounding fluid. When the fluid is air, it is named air resistance. Unlike the other resistive forces, the drag force depends on the velocity of the moving object. It is influenced by the shape and the surface area of vehicles that are exposed to air resistance directly. It is calculated by using Equation 3.5.

$$F_D = 0.5 * \rho * C_d * A * V^2 \quad (3.5)$$

Where:

F_D = Drag force
ρ = Air density (kg/m^3)
C_d = Drag coefficient
A = Frontal surface area (m^2)
V = Velocity (m/s)

The drag coefficient is a unique value for each object with different shapes. For example, based on the results of Akçelik and Besley (2003), the drag coefficients for light vehicles may vary between 0.5 and 0.65, where its range is between 0.7 and 0.9 for heavy vehicles. Table 3.2 summarizes the approximate drag coefficients of different vehicle types.

Table 3.2. *Drag Coefficient for Different Vehicle Classes (Akçelik and Besley, 2003)*

	Vehicle Class	**Drag Coefficient**
Light Vehicles	Small car	0.5
	Medium car	0.53
	Large car	0.55
	Van	0.62
	Light rigid	0.66
Heavy Vehicles	Light/Medium rigid	0.7
	Medium rigid	0.72
	Medium/Heavy rigid	0.77
	Heavy truck	0.82

3.2.1.4 Rimpull Force

Rimpull is the amount of force available between tires and ground that the engine transfers to the transmission to propel the vehicle. It is determined from rimpull-speed curves, which are provided by manufacturers. These curves also help to find out the maximum speed that a vehicle can achieve with a specific gross weight and a total resistance grade (Parreira and Meech, 2011).

Figure 3.3 represents the rimpull-speed curve of a truck with a capacity of 40 tonnes, which is used in this study. Like all the other rimpull-speed curves of trucks, this curve consists of the functions based on different gear ranges. To determine the rimpull and maximum speed, first of all, the total resistance and weight should be known and intersected on the graph. Point A represents the intersection of them.

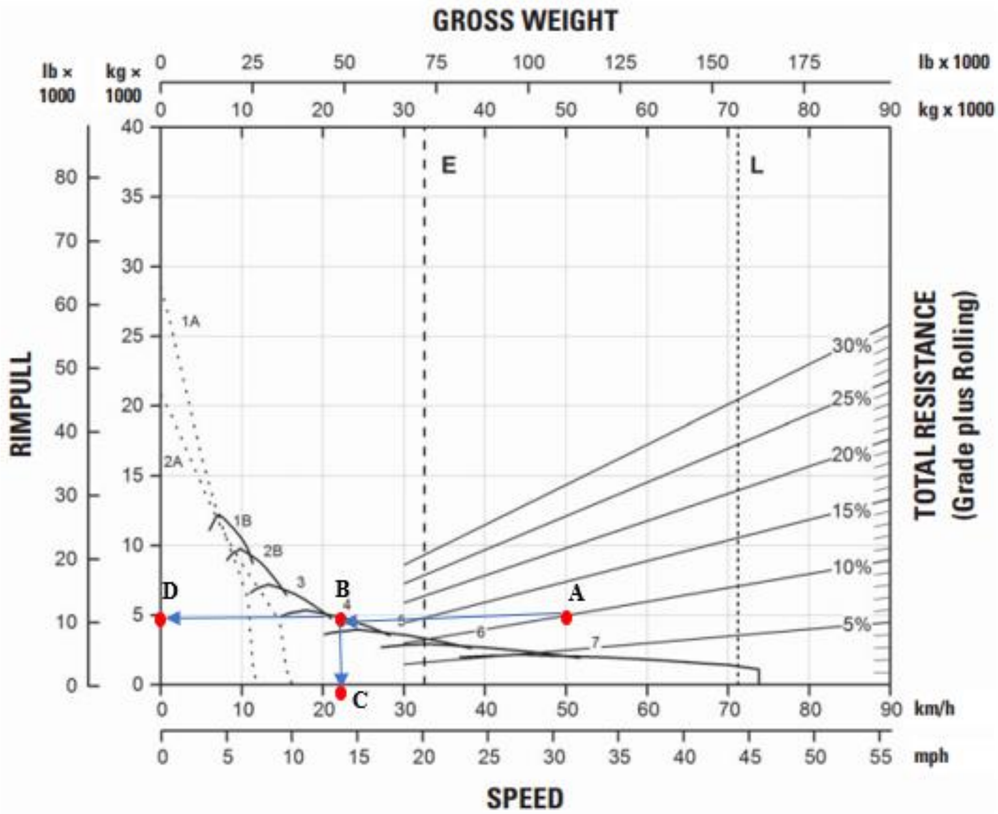

Figure 3.3. Rimpull-Speed Curve of a 40 Tonnes Truck (Caterpillar, 2014)

After finding their intersection, the point should be intersected with the rimpull speed curve and point B shows their intersection. From point B to the vertical axis, the horizontal line determines the rimpull value, which is Point D in this example. The vertical line down from point B to the horizontal axis shows the maximum reachable speed. Point C is the maximum reachable mechanical speed. For example, a loaded truck with a total weight of 50 tonnes and a total resistance of 10% can reach up to 22 km/h.

The rimpull curve of a truck with 40-tonnes capacity is digitalized with Web Plot Digitizer, and linear rimpull equations for each gear range are obtained as shown in Table 3.3. According to each speed level, rimpull is determined by using these linear equations.

Table 3.3. *Linear Rimpull Equations of a 40 Tonnes Truck*

Gear	Linear Rimpull Equations	Speed Range (km/h)
1A	R(v) = -2.227*v + 27.98	0 – 8
1B	R(v) = -0.541*v + 15.44	8 – 11
2B	R(v) = -0.393*v + 13.04	11 – 15
3	R(v) = -0.205*v + 9.53	15 - 20
4	R(v) = -0.123*v + 7.29	20 – 28
5	R(v) = -0.061*v + 5.21	28 – 35
6	R(v) = -0.058*v + 4.99	35 - 50
7	R(v) = -0.033*v + 3.53	50 - 74

Gross weight and total resistance grade affect both rimpull and maximum speed that a vehicle can reach. Total resistance is the summation of rolling and grade resistance. The maximum reachable speed is calculated from the curve by checking the gross weight (GW) and total resistance grade (TR). So, it can be written as a function in terms of these parameters. In this basis, Minitab software is used to find the function based on rimpull-speed curve. The maximum speed is determined by using Equation 3.6.

$$V_{max} = 23.88 - 0.4807 * GW + 2.711 * TR \quad (3.6)$$

According to different road grades and truck weights for each road segment, different maximum speed values can be expected considering the derived rimpull force. However, there may be a speed limit regulation in the mining area regardless of road or truck properties. In this condition, mechanically-achievable speed limits will not be regarded if their values are higher than the allowed speed limit values. Therefore, administrative speed limits for the roads in the mining area, which can serve at different purposes, will be an upper bound for the speed levels in road segments. In other words, the acceleration and braking behaviors of trucks can be performed in such a way that the minimum of administrative and mechanical speed limits for each road segment should be regarded.

3.2.2 Motion Model

The other sub-module in the algorithm considers the motion model to evaluate instantaneous movement decisions for different trucks. In this sub-module, kinematic variables (acceleration, speed, and traveled distance) per time increment are estimated to reveal the speed profiles' variations. These variables are crucial in the estimation of cycle time, unit production, and fuel consumption.

Assistive and resistive forces help to determine the instantaneous kinematic variables. The motion model is initiated by the determination of the acceleration value in the road segment. Speed and position are calculated based on the estimated acceleration values. Acceleration is the rate of change in velocity and called positive and negative acceleration in case the vehicle is speeding up and slowing down, respectively. The general formula to find out acceleration is given in Equation 3.7.

$$a = \frac{F_{net}}{M} \quad (3.7)$$

Where:

a = Acceleration for truck movement

F_{net} = Net force ($F_{assistive} - F_{resistive}$)

M = Total weight

Instantaneous acceleration and deceleration are calculated for each time interval and vary depending on the movement direction's assistive and resistive forces. Rolling resistance and drag forces are accepted as resistive forces regardless of road grade. On the other hand, grade resistance becomes dominant in calculating net force and the resultant acceleration. For flat roads, grade resistance becomes zero, and it does not affect determining the acceleration for truck movement. For the uphill movement, road grade is above zero, and it opposes the truck movement. So, it is regarded as a resistive force. When the truck moves downhill, gravitational force assists the truck motion, and it becomes an assistive force together with rimpull force. Therefore, each segment's acceleration value according to the road gradients in the movement direction can be calculated using Equations 3.8-3.10.

$$a = \frac{F_{Rimpull} - F_{RR} - F_D}{M} \quad \text{for road grade = 0\%} \quad (3.8)$$

$$a = \frac{F_{Rimpull} - F_{RR} - F_D - F_{GR}}{M} \quad \text{for road grade > 0\%} \quad (3.9)$$

$$a = \frac{F_{Rimpull} + F_{GR} - F_{RR} - F_D}{M} \quad \text{for road grade < 0\%} \quad (3.10)$$

For downhill direction, the truck weight can be good enough to sustain the truck movement if gravitational force overcomes the resistive forces. But in some cases, the weight alone may not be sufficient to initiate and maintain the movement, and rimpull force is required.

Deceleration is the opposite form of acceleration and helps to slow down the truck. Its calculation depends on the resistive forces (Equation 3.11). The minus sign in the equation represents the deceleration.

$$V_f = V_i \pm a * \Delta t \quad (3.12)$$

$$x_f = V_i * \Delta t \pm 0.5 * a * \Delta t^2 \quad (3.13)$$

Where:

V_i = Initial speed

V_f = Final speed

a = Acceleration

Δt = Time increment

By considering the estimated acceleration amounts in road segments, dynamic velocity variation in sequential time-increments are revealed with Equations 3.12 and 3.13. The velocity characterization of a truck in a road segment can be classified under three principal cases (Parreira, 2013). Each case evaluates whether a truck arrives at its maximum speed level before any deceleration (braking) decision and how long a truck can maintain a constant speed level at the maximum speed value. In the first case, the model can decide that the segment length and segment grade allow that truck to achieve its maximum possible speed and maintain this speed value for a while. In that case, the truck accelerates up to the maximum speed value, which can be from administrative limits or mechanical limits. Then, it sustains a constant speed movement for a while and starts to decelerate by calculating safe braking distance before the start point of the sequential segment. If it cannot reach its expected maximum speed level, a new maximum speed that is the value just before deceleration is calculated. Using Equation 3.14, the distance where the truck reaches its maximum speed can be calculated.

$$(V_{max})^2 = (V_i)^2 + 2 * a * S \tag{3.14}$$

Where:

V_{max} = Maximum speed

V_i = Initial speed

a = Acceleration

S = Distance to reach the maximum speed

Then, the critical distance is calculated to check if there is enough distance to safely reduce its speed at the end of the segment.

$$(V_f)^2 = (V_{max})^2 - 2 * d * CD \tag{3.15}$$

Where:

V_f = Final speed

D = Deceleration

CD = Critical distance

If the summation of S and CD is smaller or equal to segment length, the expected maximum speed can be accepted as the maximum speed. The speed profiles for Case 1 and Case 2 are shown in Figures 3.4 and 3.5, respectively. Both cases represent enough distance to reach maximum speed and brake safely to the final speed within the length of the segment.

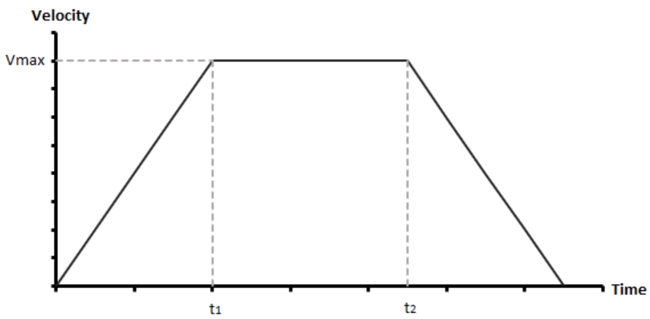

Figure 3.4. Case 1: Reaching up to Maximum Speed and Maintaining the Speed

Compared to Case 1, in Case 2, the truck immediately slows down just after reaching up to the maximum speed. In Case 1, the truck is driven at a constant speed that equals the maximum speed for a certain time.

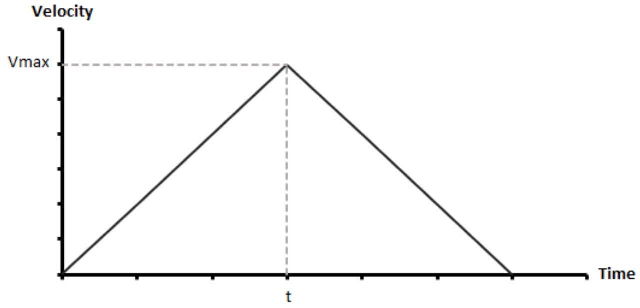

Figure 3.5. Case 2: Reaching up to Maximum Speed and Then Deceleration

If the summation of S and CD is larger than the segment's length, the model applies Case 3 and needs to calculate a new maximum speed that is smaller than the expected maximum value. Here, there is no sufficient distance for the truck to reach its maximum speed, or the truck cannot reduce its speed safely after reaching the maximum speed. For this reason, first of all, the distance to get maximum speed (S) is calculated as given in Equation 3.16. Then, a new reduced maximum speed is determined by using Equation 3.14. The speed profile that can be seen in Case 3 can be examined in Figure 3.6.

$$S = \frac{V_f^2 + 2 * d * x - V_i^2}{2 * d + 2 * a} \tag{3.16}$$

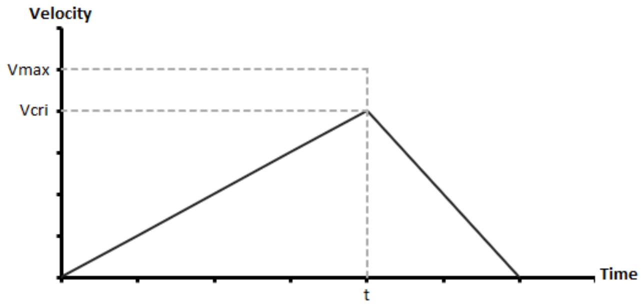

Figure 3.6. Case 3: Maximum Speed cannot be Achieved

The speed profiles shown in Figures 3.4-3.6 assume that the truck starts accelerating from 0 km/h at the beginning of the segment. In addition, these figures assume that velocity is reduced to zero at the end of the segment. However, in practical applications, a truck does not have to stop at each segment's end. If there is no intersection point of the road network where a truck needs to decelerate before that point, this truck can transfer its final speed at the end of the segment as an initial speed value of the sequential segment. On this basis, the model checks the intersection points, and deceleration (braking) requirements are evaluated when constructing speed profiles.

3.2.3 Fuel Consumption Calculation Model

In the developed model, fuel consumption is calculated by using a microscopic model. As mentioned in Chapter 2, microscopic models estimate fuel consumption rates more accurately but need more detailed data with higher complexity. Bektaş and Laporte (2011) developed a mathematical model to calculate fuel consumption by using the microscopic modeling approach. Road conditions and truck properties in the model significantly impact fuel consumption calculation, and they are introduced as input data. In the formulations, there are also some deterministic values specific to road conditions and truck properties, which are denoted as α and β, respectively. Calculations of α and β are shown in Equations 3.17 and 3.18.

$$\alpha_{ij} = a + g * \sin\theta_{ij} + g * C_r * \cos\theta_{ij} \quad (3.17)$$

Where:

a = Acceleration (m/s^2)
g = Gravitational constant (m/s^2)
C_r = Rolling resistance coefficient
θ_{ij} = Angle of road segment from i to j

$$\beta = 0.5 * C_d * A * \rho \quad (3.18)$$

Where:

C_d = drag coefficient

A = frontal surface area of truck (m^2)

ρ = air density (kg/m^3)

The total energy consumption between nodes (P_{ij}) in a segment can be calculated with Equation 3.19.

$$P_{ij} = \alpha_{ij} * (w + f_{ij}) * d_{ij} + \beta * d_{ij} * V^2 \quad (3.19)$$

Where:

w = Empty truck weight (kg)

f_{ij} = Payload transported between road segment from i to j (kg)

d_{ij} = Length of segment (m)

V = Speed of truck (m/s)

The amount of fuel consumed on the road segment can be determined by converting the energy requirement to the consumed fuel amount as given in Equations 3.20 and 3.21 (Bektaş and Laporte, 2011).

$$3{,}600{,}000 \text{ Joules of energy} = 1 \text{ kWh of energy} \quad (3.20)$$

$$8.8 \text{ kWh of energy} = 1 \text{ Liter of fuel} \quad (3.21)$$

Trucks consume more fuel while driving uphill compared to a movement downhill since there are more resistive forces to be overcome in uphill driving. The calculations given in Equations 3.17-3.21 estimate the fuel consumption on a segment where its gradient is greater than or equal to zero. With the help of road grade, gravitational force might be sufficient for the movement in a downhill direction. In these situations, the engine produces an idling power, and the idling fuel consumption rates are considered (Parreira, 2013). Besides, idling fuel consumption is also considered when the truck waits in the queue in the loading and the dumping locations.

The model checks the fuel tank level whenever the truck dumps its material and becomes unloaded (empty). The model calculates the amount of fuel consumed in every segment, and the fuel tank level is reduced simultaneously. If the fuel tank level is below 10% of its full capacity, the truck is generally assumed to have a refueling service.

3.3 Development of the Discrete-Event Simulation Algorithm

Simulation can be defined as the imitation of a real system's operations over time, usually using computer software. It is the process of mimicking and evaluating the real-world system model's behavior under the given conditions with numerical experiments. The main reason for using simulation is that it can examine not only simplified systems but also complicated systems easily. In addition to that, there are many benefits of using simulation modeling. First of all, systems with high-risk activities and critical situations could be studied in a safe environment without risk. It serves to reduce mistakes and improve results by showing the consequences of actions. Another benefit of using simulation is that impacts of different scenarios can be easily evaluated and identified by changing the variables. Therefore, it provides a better understanding of how variables affect the results. However, there are some disadvantages of simulation, such that it may be expensive and time-consuming due to higher computing power requirements and the expense of software licenses (Kelton, 2004).

Simulation models can be classified into three following categories (Banks *et al.*, 2010):

i. Static vs. Dynamic Simulation Models: Static simulation models represent a system at a particular time and are not affected with time, while dynamic simulation models examine a system whose state changes over time.

ii. Deterministic vs. Stochastic Simulation Models: Deterministic simulation models do not have any random variable or have a random variable(s) that has a very negligible effect on simulation results. On the other hand, stochastic models have at least one random variable as an input with an observable impact on simulation dynamics.

iii. Continuous vs. Discrete Event Simulation Models: In continuous models, the system state changes continuously as a function of time. It means that there is a requirement to monitor the system state in pre-defined time increments. In discrete event models, the system state can change only at a discrete set of time points. Their graphical representations are shown in Figure 3.7.

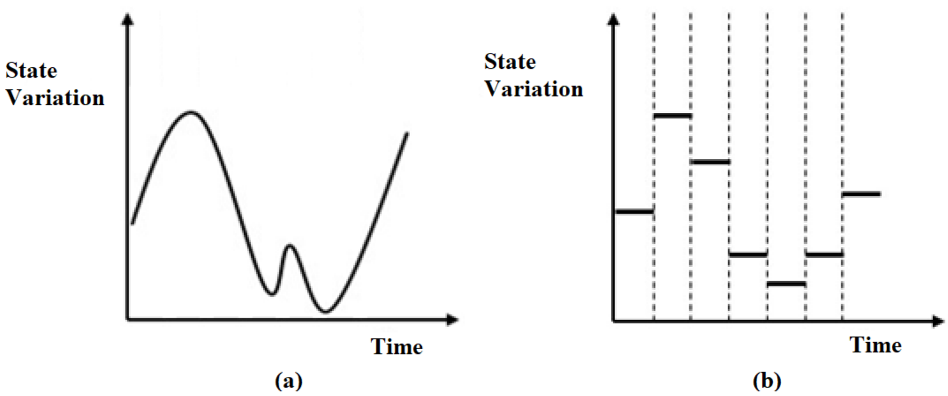

Figure 3.7. Continuous (a) and Discrete Event (b) Simulation Models

In this research study, the developed simulation model is considered to be a dynamic, stochastic, and discrete event model. It is possible to reflect these stochastic and dynamic features of mine haulage systems to the simulation model using the Arena simulation environment, which is discrete-event simulation software. For this reason, Arena, which is based on SIMAN simulation language, is used to model mine haulage system for evaluating the fuel consumption of trucks. Simulation models are created by using flowchart modules and data modules to represent the system's processes. Flowchart modules are a set of objects which are placed for describing the simulation process, where data modules define the characteristics of process elements such as values and expressions of entities and resources. Among data modules, the followings are defined in the computational environment to simulate the mine haulage system:

- Entity: Entities are defined as the dynamic objects of the simulation. The simulation starts with creating entities, and they are continuously active through the system until the end of the simulation.
- Variable: Variables reflect the specifications of the overall system regardless of the defined entities.
- Attribute: Attributes are unique to entities themselves and define the characteristics of entities individually.
- Resource: Resources are used by entities and have an impact on how an entity behaves in the observation period. They have limited capacities. Therefore, if an entity seizes an unavailable resource, it must wait in a queue until the required resources become available.
- Queue: Queue is the holding point of entities whose progress is constrained due to limited or unavailable resources. There are different ranking rules used when defining queue conditions. First In, First Out is the default ranking rule in Arena.
- Schedule: It is defined as the operating schedule for resources.

In this research study, trucks are considered as active entities as a part of the mine haulage system. There are also three different entity types for each excavator. In the model, excavators and crushers are introduced as resources that they may be seized by a truck, delayed for loading and dumping processes, and released to the next station in the system. In addition to that, the fuel station and parking station are other resources for the model's refueling and parking processes. Segment properties, truck characteristics, and weather and road conditions are considered as system variables in this research study. Forces, kinematic variables like acceleration, deceleration, and speed levels, cycle times, payload, and the amount of fuel consumed are regarded as attributes. Each attribute value is captured and stored for each individual truck. The flowchart modules that are used extensively in the modeling phase can be viewed in Table 3.4.

Table 3.4. *Flowchart Modules and Definitions*

Flowchart Module	Name	Definition
	Create	Starting point of entities
	Dispose	Ending point of entities
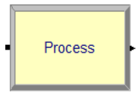	Process	Main processing method. It contains the seize, delay, and release processes
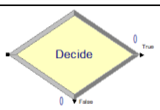	Decide	Decision-making process based on conditions or probabilities
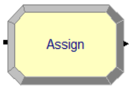	Assign	Assigning new values to variables, entity attributes
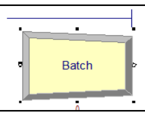	Batch	Grouping entities based on the number of entering entities or attribute
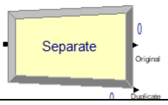	Separate	Splitting batched entities or duplicating entities
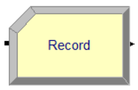	Record	Collection of statistics
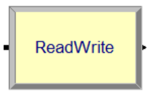	Read Write	Reading data from an input file and writing data to an output file
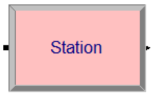	Station	Physical or logical location where processing occurs
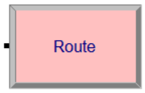	Route	Transferring entities between stations

As shown in Figure 3.8, the simulation starts with creating truck entities using the Create module. Trucks with different specifications are built from individual Create modules. Then, each group of trucks is assigned to a specific excavator that can be operated in either waste or ore excavation in different locations of the pit. Truck entities from other Create modules are combined. The cumulative information is transmitted to the Decide module to initiate the truck cycle toward the assigned excavator for the loading process. Assign modules are used to assign specific attributes to entities and variables in the system. The road between stations is divided into road segments according to grade levels and intersection points. The traveling characteristics of each truck entity will be different from each other. Therefore, each segment number is considered as an attribute. The specific route and segment attributes for each truck entities are assigned when trucks move through the Assign modules. For example, at the beginning of the simulation, all trucks are located in the parking area, and they travel to the next station from this parking area. Additionally, a specific number is defined for each truck entity to enable simultaneous monitoring outputs of individual trucks along the route and segment.

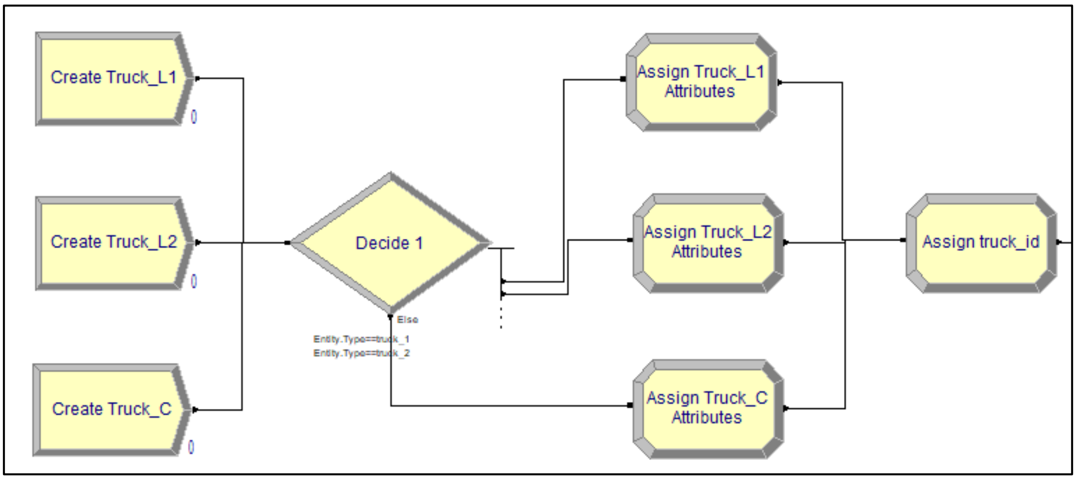

Figure 3.8. Creation of Truck Entities and Excavation Assignment

The first part of the 'Hauling Submodel' can be seen in Figure 3.9. In this submodel, speed levels and hauling time are determined by using segment information of routes such as length, grade, and location of intersection points. The submodel starts with the weather forecasting according to rain probabilities based on monthly precipitation input. Coefficient of rolling resistance changes if rainy weather is detected. For each day, a new probability of precipitation is determined. After that, the simulation continues with the calculation of forces and kinematic variables such as acceleration, deceleration, and the maximum speed that a truck can reach by using the related equations mentioned in Section 3.2.

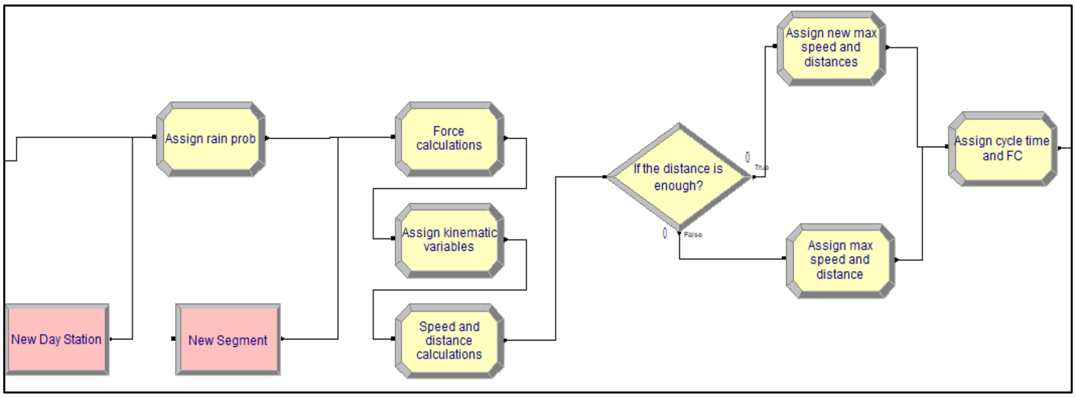

Figure 3.9. Hauling Submodel – Part 1

In Assign modules, these calculations change depending on whether road grades are in an uphill or downhill direction since force calculations and kinematic variables are drastically affected by road grades and directions. The maximum speed level is checked by including both the mechanically achievable speed limit of trucks in the available road segment conditions and the mine speed limits. Each time, the algorithm considers the minimum of these values when deciding on the final speed active in the segment. Then, the road segment's speed profiles are generated by calculating the initial and final speed level according to segment lengths and enforcements of segment connection points. Suppose the end of the road segment is an intersection point where a truck needs to lower its speed to zero. In that case, the truck revises all the acceleration and deceleration decisions accordingly. Otherwise, the segment's final speed will be transmitted to the sequential segment as the initial speed.

Decide module figures out whether the truck can reach a maximum speed level or not by checking the acceleration and braking distances. Suppose the summation of these distances is equal or less than the length of the segment. In that case, two conclusions can be drawn: i) There is enough distance for both reaching up to the calculated maximum speed, and ii) braking safely to the final speed within the length of the segment. If the summation of acceleration and braking distances is greater than the segment length, then the model revises its maximum achievable speed level in the segment so that acceleration and braking can be adequately performed. The travel time of each road segment and the amount of fuel consumed are determined in this submodel.

After estimating the segment's speed levels and fuel consumption, the model checks whether the route is completed. If completed, the model returns to New Segment Station, and the segment number is incremented by one in the Assign module until the ending of each route. This incrementation is performed once the required truck calculations for the active segment is completed. At the end of the route, truck entities that complete the 'Hauling Submodel' proceeds to their destination stations. Figure 3.10 shows the second part of the 'Hauling Submodel' that decides the following station. Route modules are used to transfer entities between the pre-specified stations. On this basis, the movement of trucks from the parking area to the excavator stations is achieved first. Station modules point out the locations of excavators, crushers, parking areas, and fuel stations and refer to destination points in and around a pit.

Figure 3.11 represents the loading processes performed by two excavators (Exc_L1 and Exc_L2) in the limestone mine and one excavator in the clay mine (Exc_C). Each loading submodel for three excavators follows the same principles. The submodel starts with the Station module, which points to the excavator location. When a truck entity arrives at an excavator, the model checks whether that excavator is occupied or not by using the Decide module. If the excavator is busy with loading another truck, the inbound truck entity needs to wait in the loading queue. The ranking rule of the queue is in terms of First in First Out. It means that the last incoming truck entity passes to the end of the queue and waits for the other trucks in the queue to be loaded for its turn. If the excavator becomes available, it starts to load the truck entity at the forefront of the queue after a truck maneuvering time.

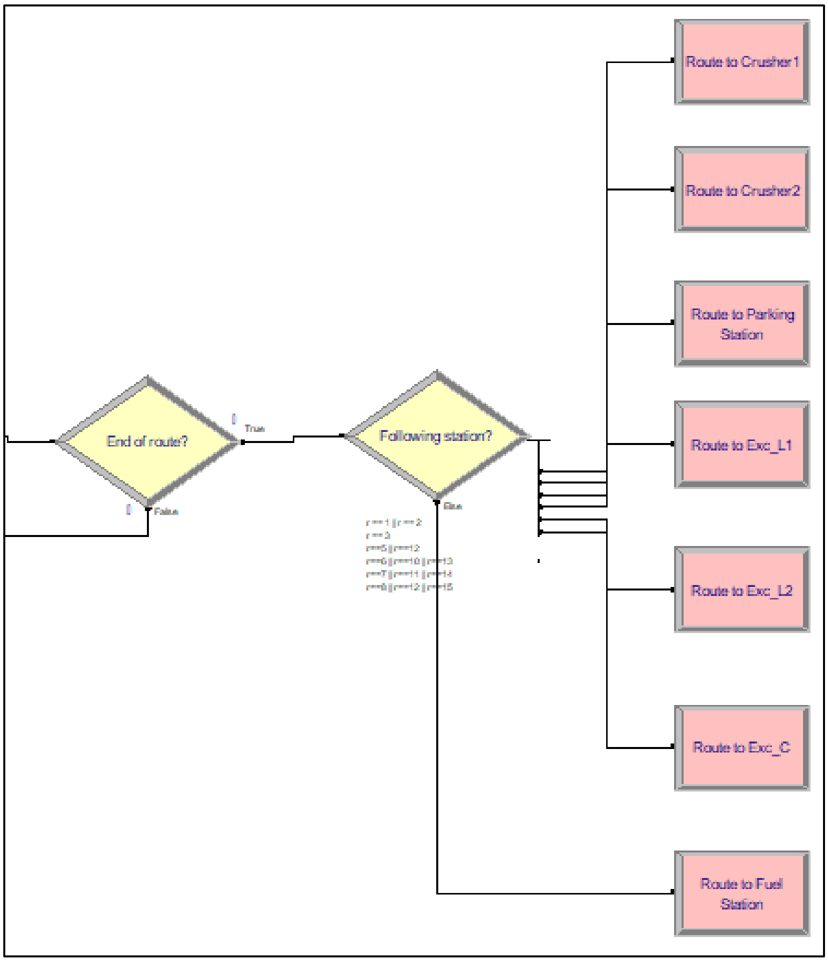

Figure 3.10. Hauling Submodel – Part 2

Loading time is assigned in the Process module, and it is used to manage and activate the loading process. After the loading process is completed, then the truck is labeled as loaded in the algorithm. Following the loading operation completion, a new truck weight is assigned randomly regarding the material load distribution. Fuel consumption of truck during the loading process is also calculated in the Assign module. At this point, the fuel consumption rate is estimated, assuming that truck engines are operating in the idling condition during loading and queueing periods.

Loaded trucks are allowed to travel only in the route(s) between excavators and dumping destinations. Any route change is not allowed in the algorithm until the hauled material is not dumped. Therefore, the Route module is used to transfer loaded truck entities to either crusher or waste dumpsite station.

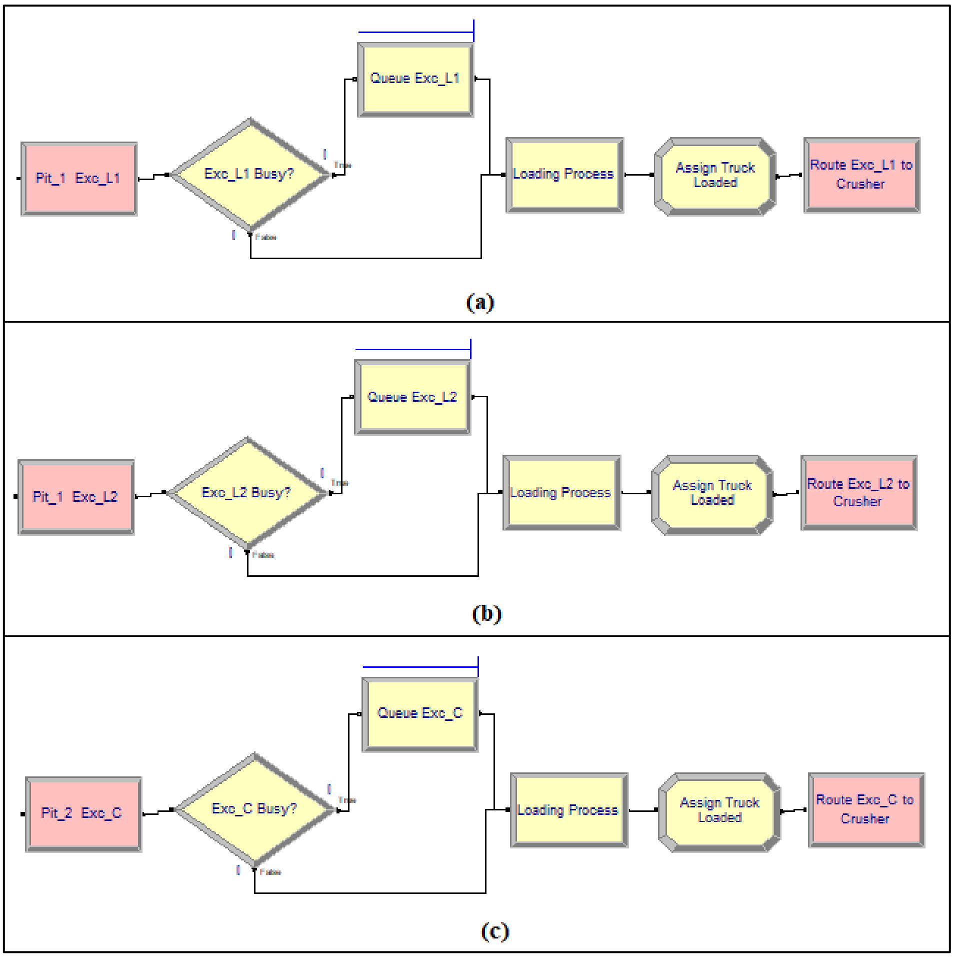

Figure 3.11. Loading Processes of Exc_L1 (a), Exc_L2 (b), and Exc_C (c)

As discussed previously, the 'Hauling Submodel' observable in Figures 3.9 and 3.10 is also used to allocate truck entities from excavators to crusher or dumpsite. Speed levels and hauling times of each road segment are recorded for the generation of speed profiles and the calculation of cycle times. The amount of fuel consumed is also calculated cumulatively for each segment and route to reveal trucks' sectional and total fuel consumption profiles.

The flowchart of the dumping process in the crusher area can be examined in Figure 3.12. A dumping station that can be either of dumpsite or crusher needs to be assigned for all trucks whose loading process can be performed by multiple excavators. Following a travel in the given route, if there is a dumping point occupied by another truck, any incoming truck should stop at the queue's back. The dumping time is introduced to the cycle times of dumping trucks. After the dumping process, trucks are labeled as empty.

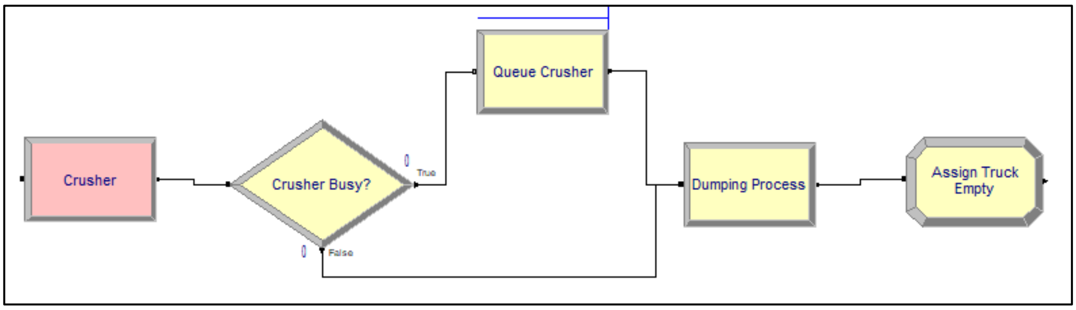

Figure 3.12. Crusher Dumping Process

Similar to the Loading Process, fuel consumption during any dumping operation is determined in the Assign module by including the idling conditions of trucks. Just after the dumping process, the model checks the sequential potential destinations and routes. There are three possible destinations as i) turning back to the excavator in pits for the loading process, ii) traveling to a fuel station for a refueling process, and iii) traveling to a parking station due to an administrative, lunch, or shift break. First, the model checks the fuel level of the fuel tank. It is assumed that the algorithm decides for a refueling process if the fuel level in the tank is below 10 percent of its total capacity. This threshold value is adjustable in the algorithm. The queue situation is also considered in the fuel station. If there is a queue, trucks need to wait for the refueling process. The fuel tank capacity becomes full after the refueling process, and trucks are ready to proceed to the following station. The control of the fuel tank level and the refueling step requirements are shown in Figure 3.13.

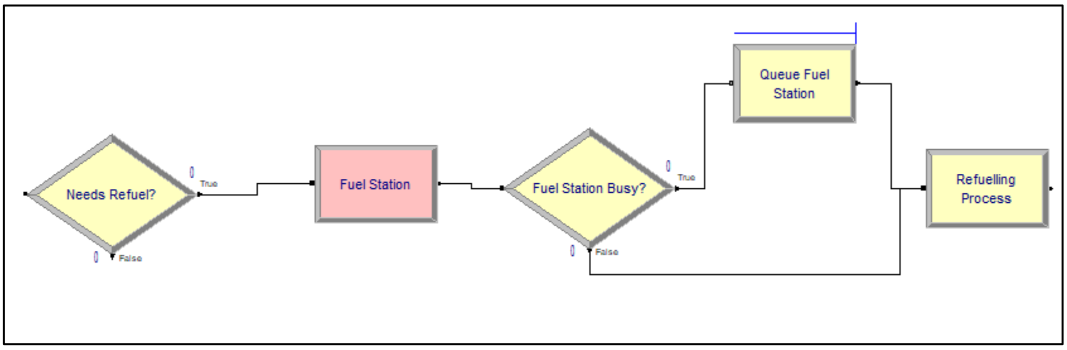

Figure 3.13. Refueling Process

Whenever the Decide module gives an adverse decision for refueling, the administrative breaks are controlled, as shown in Figure 3.14. First, the model checks if there is a shift break or not. If a break is detected, truck entities are forced to move to the parking station. The Batch module is used for recalling all empty truck entities, and no operation is permitted throughout the break duration. On the other hand, the loaded truck entities cannot take a break without dumping their loads. After completing the shift break, trucks are transferred from the parking station to the corresponding excavator stations by using Hauling Submodel.

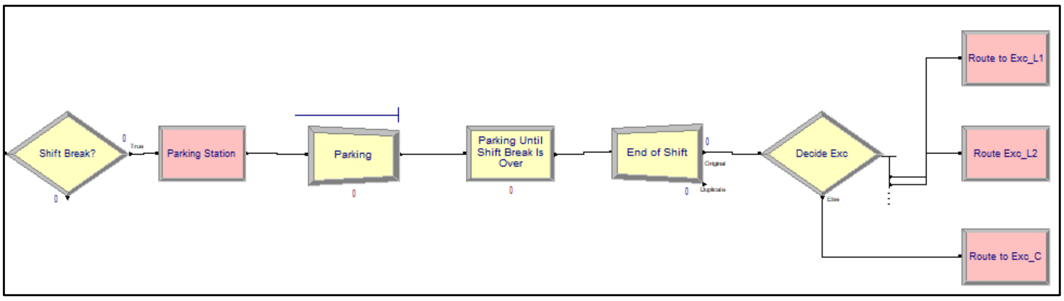

Figure 3.14. Break Time Control

If there is no shift break, the model controls whether shift will be over anytime soon. If the shift end is not detected, trucks are allowed to hold their scheduled production cycle by proceeding with a new route. Suppose the shift is confirmed to be ended very soon; the algorithm also checks whether it has been a year since the beginning of the simulation or not. At this point, the algorithm's default settings simulate the model for a one-year operation. This target observation period is adjustable in the algorithm. If the target period is not completed in the simulation, trucks are moved to the parking station at the end of the last shift and wait for the new operation day. All the simulation outputs covering daily production and fuel consumptions are recorded and reported in detail, considering the fuel consumption rates in segments and routes individually and cumulatively for each truck and truck fleet. When a new operation day starts, trucks travel to their assigned excavators and initiate their production schedule regarding daily weather information.

On the other hand, if the simulation detects that the target observation period, which is one year as default, is over, the simulation ends. The simulation is replicated until the simulation outcome reaches a balance point. At the ends of the simulation replications, an output data file is obtained where the values are printed on shift-, day-, and period-basis. Figure 3.15 represents the model's control mechanism regarding the shift ends and the target observation period.

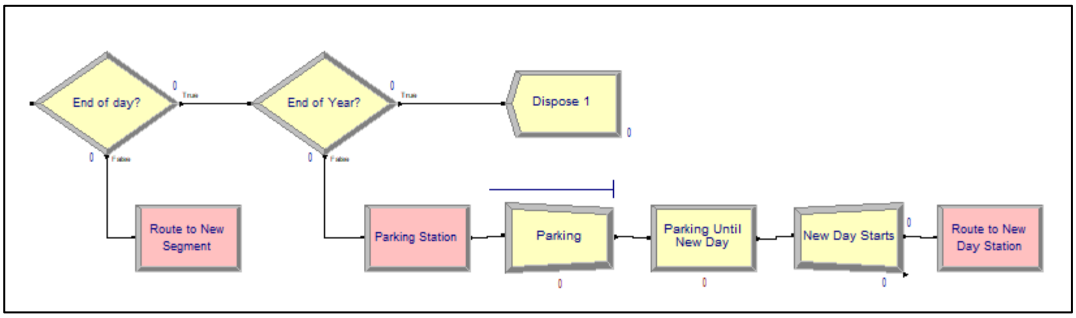

Figure 3.15. Decisions for Shift Ends and Target Observation Period

All the possible routes where a truck can travel between multiple points in a mining area with different operational intentions were modeled using Arena discrete event simulation software. On this basis, dynamics interactions between the ground and vehicles were introduced into the model, and interactive acceleration and deceleration decisions were achieved according to the route segment and weather information and precedence dependencies between the segments. The developed algorithm allows monitoring fuel consumption rates simultaneously for individual vehicles and the fleet itself. The algorithm entails developing various submodels called Hauling, Loading, Dumping, Refueling, and Parking. In the next chapter, applying this model into a case study for a cement company is explained and discussed using both deterministic and stochastic inputs.

CHAPTER 4

IMPLEMENTATION OF THE MODEL FOR THE HAULAGE SYSTEM OF A CEMENT COMPANY

4.1 Introduction

This chapter presents the application of the developed model using data provided by a cement company. In Chapter 4.2, a detailed explanation of the study area and input dataset provided by the company will be given. The implementation results will be discussed in Chapter 4.3.

4.2 Study Area and Data Acquisition

The model is applied for the hauling operations performed jointly in two mines by a cement company in Bolu province. Limestone and clay are extracted separately in these mines to meet the cement plant's raw material requirement, located in between the mine sites. After drilling and blasting operations in the mining areas, limestone and clay materials are loaded into trucks and transported directly to the processing plant for a crushing process. This research study aims to analyze the fuel consumption profile of the hauling trucks that operate between the multiple locations of various operational intentions in the cement company's license area.

The mines operate 29 trucks, each having a payload capacity of 40 tonnes and an empty vehicle weight of 34 tonnes. It has a fuel tank capacity of 530 L and its frontal surface area is 15 m^2. These vehicle specifications will be included in assistive and resistive force calculations and refueling decisions. Relative positions of the clay mine, the limestone mine and the processing plant can be viewed in Figure 4.1. The limestone mine, which operates in one shift with 8- working hours per day and produces 4,500 tonnes of material, is located nearly 16 km away from the processing plant. In the mine, 2 excavators and 22 trucks are used for haulage operations. On the other hand, the clay mine is located approximately 7.58 km away from the processing plant and achieves 1,200 tonnes of production per day with one shift a day. 1 excavator and 7 trucks are employed in the material loading and hauling operation. Variation of road grades in the routes from the limestone and the clay mines to the processing plant can be investigated in Figure 4.2.

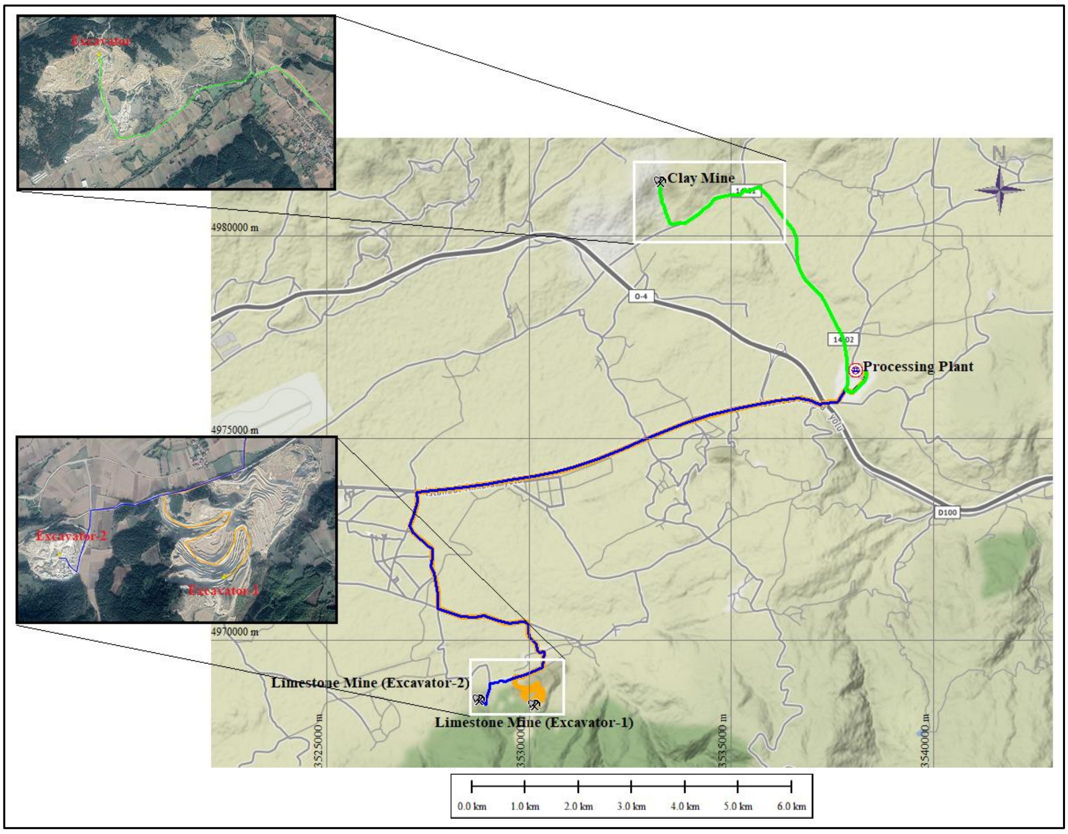

Figure 4.1. Haulage Routes between the Mine Sites and the Processing Plant

Each route between the hauling operation's destination points was subdivided into road segments with similar grade info. For instance, the route from the clay mine to the process plant, shown in Figure 4.2 (b), contains ten different sequential road segments (Table 4.1). Here, a track length where is not any drastic or significant variation in road grade is considered to be one segment.

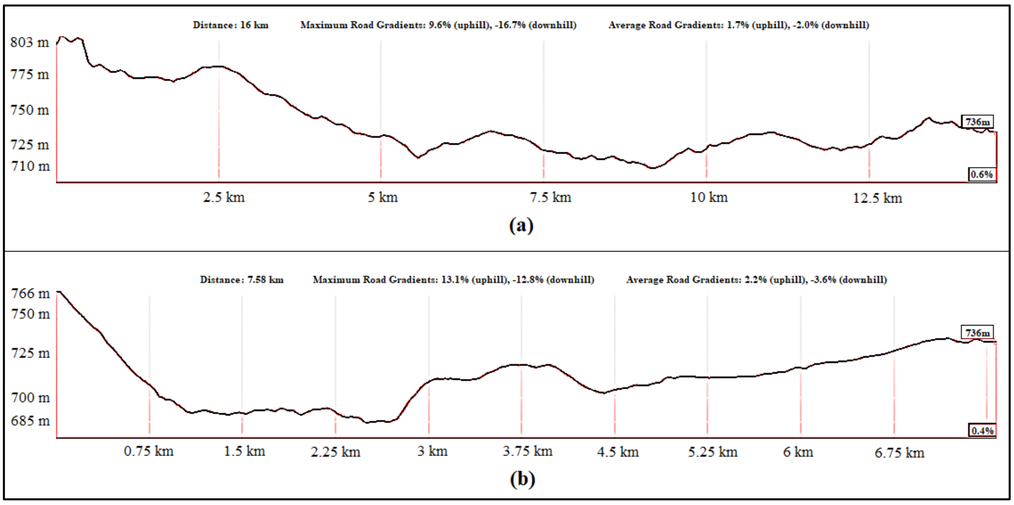

Figure 4.2. Road Profiles from the Limestone (a) and Clay Mines (b) to the Plant

In Table 4.1, positive signs in the road grade values refer to uphill movement, while negative signs point to downhill movement with gravity's assistive force. The intersection column shows how a vehicle should act at the end of each segment in the given direction. In this sense, three intersection codes were defined in the model.

Table 4.1. *Road Segment Info of the Route from the Clay Mine to the Plant*

Route (from the Clay Mine)				
Segment ID	**Length (km)**	**Road Grade**	**Road Type**	**Intersection**
$S_{5,1}$	1.14	- 4.00°	3	1
$S_{5,2}$	1.06	0.00°	2	1
$S_{5,3}$	0.33	- 1.72°	2	1
$S_{5,4}$	0.20	0.00°	2	1
$S_{5,5}$	0.37	3.86°	1	0
$S_{5,6}$	0.30	0.00°	1	0
$S_{5,7}$	0.60	1.50°	1	0
$S_{5,8}$	0.40	- 4.24°	1	0
$S_{5,9}$	2.80	1.22°	1	1
$S_{5,10}$	0.38	0.00°	4	2

In case that the active segment holds an intersection code of 0 (zero), it means that the vehicle may pass to the sequential segment without any need of braking. Therefore, the ultimate speed achieved at the segment end will be the sequential segment's initial speed. If the segment is ending with an intersection and if the vehicle should stop at the segment end, it takes the value of 1 (one). It means that the right of way belongs to the vehicles traveling on the other intersecting road. In this situation, vehicle moving on this segment should choose a speed and distance to initiate deceleration in such a way that its final speed at the end of the segment should be zero. Last, a segment with an intersection value of 2 (two) refers to the last segment in the active route where vehicle speed should be zero at the segment end.

On the other hand, the road type values refer to different road types where different coefficients of rolling resistance are available. At this point, four road types were defined in the model. Table 4.2 summarizes the rolling resistance coefficients of dry road surfaces (Kaufman and Ault, 1977), and allowable speed limits of these road types introduced in the algorithm.

Table 4.2. *Speed Limits and Rolling Resistance Coefficients for Road Types*

Road Code	**Road Type**	**Rolling Resistance Coefficient**	**Speed Limit (km/h)**
1	Asphalt Roads	0.02	40
2	Rural Roads	0.03	30
3	In-Mine Roads	0.05	20
4	In-Plant Roads	0.03	10

The coefficient of rolling resistance can change depending on the weather condition. In this model, the probability of daily precipitation is determined depending on the monthly rainy-day data. The rolling resistance coefficient for wet road surfaces is 30% greater than in the dry surfaces while driving at a speed of 30 km/h (Ejsmont *et al.*, 2015). In the model, the coefficient of rolling resistance for a rainy day is calculated accordingly. Table 4.3 tabulates the temperature and days with the Bolu province's precipitation statistics taken from the Turkish State Meteorological Service (2020). The raining probability is determined with the ratio between the rainy days and the total number of days in months. In the simulation environment, it will be assigned as a binary variable, 0 or 1. If it takes a value of 1, it means that the active day is rainy or vice versa. Precipitation probability for the individual days will be assigned randomly depending on the related month's raining probability.

Table 4.3. *Monthly Weather Statistics of Bolu Province*

Month	**Average Temperature (°C)**	**Days with Precipitation**	**Probability of Rain**
January	0.4	15.6	0.50
February	1.7	14.4	0.51
March	4.7	14.6	0.47
April	9.6	13.3	0.44
May	14.0	14.0	0.45
June	17.3	11.7	0.39
July	19.8	6.2	0.2
August	19.8	5.3	0.17
September	16.1	7.1	0.24
October	11.7	10.6	0.34
November	6.9	12.0	0.4
December	2.6	14.8	0.48

The cement company, called the processing plant or crusher in this study, is located between the mines. Once a truck arrives at the processing plant, it may follow different routes around the plant according to various operational requirements (Figure 4.3). Considering both the mines and the destination points around the plant, there are seven different stations defined as resource data in the algorithm model. These are Excavator-1 in the Limestone Mine (LM1), Excavator-2 in the Limestone Mine (LM2), Excavator in the Clay Mine, Limestone Crusher (Crusher1), Clay Crusher (Crusher 2), Fuel Station, and Parking Station. As seen, Crusher 1 and

Crusher 2 are allocated for the material hauled from the limestone and clay mines, respectively. Since the crushers are located close to each other, the intermediate distance is negligible. Therefore, the routes from the crushers to the next stations are considered identical for both crushers.

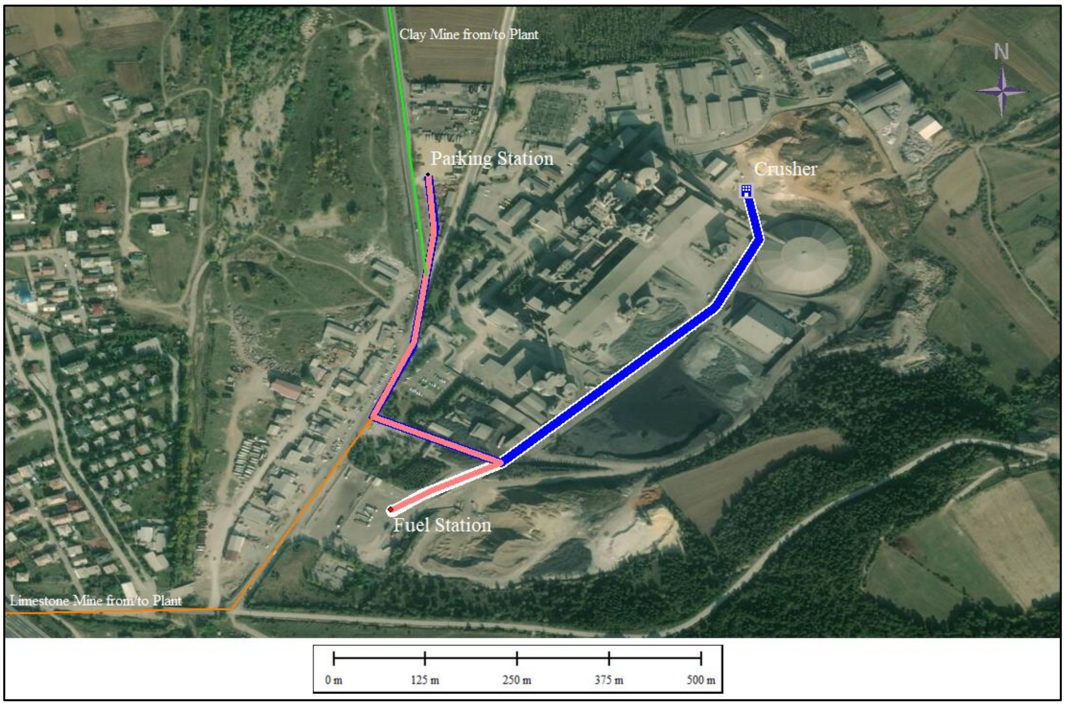

Figure 4.3. Truck Destinations around the Processing Plant

The stations enable the construction of 12 different routes used in the simulation of the mine haulage system. Therefore, a truck may travel in one of the routes between: i) Excavator-1 in the Limestone Mine (LM1) and the Crusher1, ii) Excavator-2 in the Limestone Mine (LM2) and the Crusher1, iii) Excavator in the Clay Mine (CM) and the Crusher2, iv) Parking Station and Excavator-1 in the Limestone Mine (LM1), v) Parking Station and Excavator-2 in the Limestone Mine (LM2), vi) Parking Station and Excavator in the Clay Mine (CM), vii) Crusher and Fuel Station, viii) Crusher and Parking Station, ix) Fuel Station and Parking Station, x) Fuel Station and Excavator-1 in the Limestone Mine (LM1), xi) Fuel Station and Excavator-2 in the Limestone Mine (LM2), and xii) Fuel Station and Excavator in the Clay Mine (CM). Details of the potential routes used in the simulation can be observed in Table

4.4. These routes were subdivided into segments. Each segment's precedence affects the dynamic speed decisions that can be either of acceleration, deceleration or constant speed. Segment details of the route between the clay mine and crusher2, where its route ID is 03 and segment info is recorded in $S_{3,j}$, were already shown in Table 4.1. Segment information of the other routes can be examined from the tables in Appendix A.

Table 4.4. *The Routes used in the Material Haulage Operations*

Route ID	Route	Route Length (km)	Road Segments (#)
1/2	LM1 to/from Crusher1	16.00	13
3/4	LM2 to/from/ Crusher1	15.95	13
5/6	CM to/from Crusher2	7.58	10
7	Crusher1,2 to Parking Station	0.62	4
8	Crusher1,2 to Fuel Station	0.97	4
9	Fuel Station to Parking Station	0.61	3
10	Fuel Station to LM1	15.77	14
11	Fuel Station to LM2	15.72	14
12	Fuel Station to CM	6.61	9
13	Parking Station to LM1	15.64	14
14	Parking Station to LM2	15.59	14
15	Parking Station to CM	7.34	11

As seen in Table 4.4, the vehicles perform their travels between the points at the loading points in mines, crushers, parking station, and fuel station. In the final destination points, trucks also spend some time in a stationary position during the loading, dumping, and refueling activities. Stochastic characterization of these periods was achieved using a survey applied to the truck operators. In the survey, minimum, maximum, and most likely time values were asked to determine the triangular distributions of the related fields (Table 4.5). In the values, the loading time includes spotting time where the dumping time includes maneuvering time for dumping.

Table 4.5. *Time Statistics at the Destination Points*

Truck Type	**Loading Time (min)**			**Dumping Time (min)**			**Refueling Time (min)**		
	Min	Most Likely	Max	Min	Most Likely	Max	Min	Most Likely	Max
Truck_L1	1.42	2.08	3.33	0.75	0.92	1.67	9	12	19
Truck_L2	1.42	2.08	3.33	0.75	0.92	1.67	9	12	19
Truck_C	1.17	1.92	3.08	0.67	0.83	1.83	9	12	19

According to the truck's operating specifications, its nominal and maximum payload capacities are 38.2 and 42 tonnes, respectively. The payload amount carried by the truck is expected to vary between these capacities after each loading activity. Therefore, normal distribution functions were defined separately for the loading operations in the mines. In this sense, using the expert opinions, the payload distribution functions were determined with an expected value of 38.2 tonnes and the standard deviations of 0.93 and 1.27 tonnes for the limestone and clay mines, respectively (Figure 4.4). At this point, the payload values in the simulation model will be assigned randomly between 36.34 and 40.06 tonnes, and 35.66 and 40.74 tonnes in 95.5 percent confidence interval for the mines, respectively.

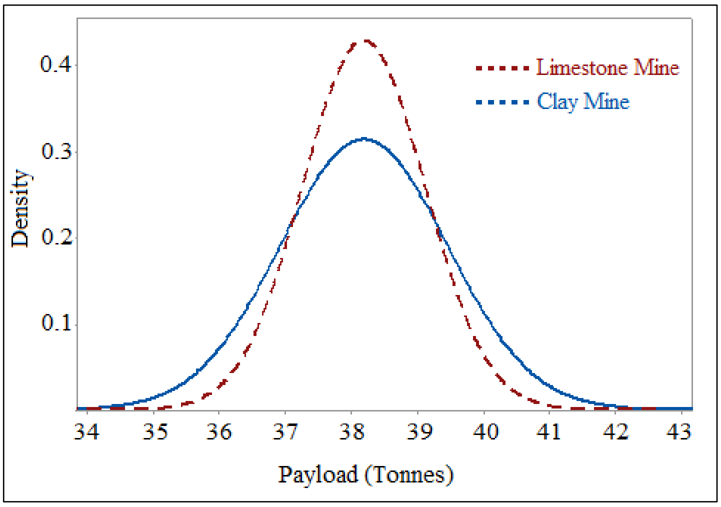

Figure 4.4. Payload Data Distribution Functions of the Mines

The mine is operated in one 8-hour shift a day. There is a scheduled one-hour lunch break at the mid-shift. On this basis, the operators drive their trucks to the parking station 4 hours after the shift start. If the truck is loaded, the driver moves to the parking station only after dumping the loaded material. Therefore, some drivers may arrive late for the lunch break. Following the break, trucks resume the production schedules until the end of the shift. Trucks move to the parking station at the shift end.

4.3 Implementation of the Model

The simulation algorithm discussed in Section 3.3 was implemented using the cement company dataset given in Section 4.2. In this sense, the simulation outputs were captured and stored daily, monthly, and annual basis for individual trucks to reveal their speed and fuel consumption behaviors. Many parameters affect the amount of fuel consumed, such as payload, velocity, road grade, road condition, and weather condition. Their effects on fuel consumption will be discussed.

4.3.1 Effect of Precipitation Rate

Weather condition is one of the parameters that are hard to control and measure. However, it needs to be included in fuel consumption studies since it affects the ground's resistive force and the resultant fuel rate. Therefore, monthly precipitation probabilities of the territory are included in the model. Figure 4.5 represents the variations in the expected daily fuel consumption values of individual trucks for the limestone and clay mines, regarding a total of 8-hour shift a day. There are 22 trucks operated between the limestone mine and the process plant, and their average fuel consumption values show differences for each month. It is observed from the figure that the maximum and minimum fuel consumptions in the limestone trucks are expected to be in April and July with the values of 90L per day and 82L per day, respectively. On the other hand, seven trucks are operated in the clay mine. The maximum and minimum daily fuel consumptions are also expected to be observed in April and July for the clay mine with the values of 88L per day and 83 L per day, respectively. Since the route characteristics between the mines and the plant are different, daily fuel consumptions of trucks for the mines show a change.

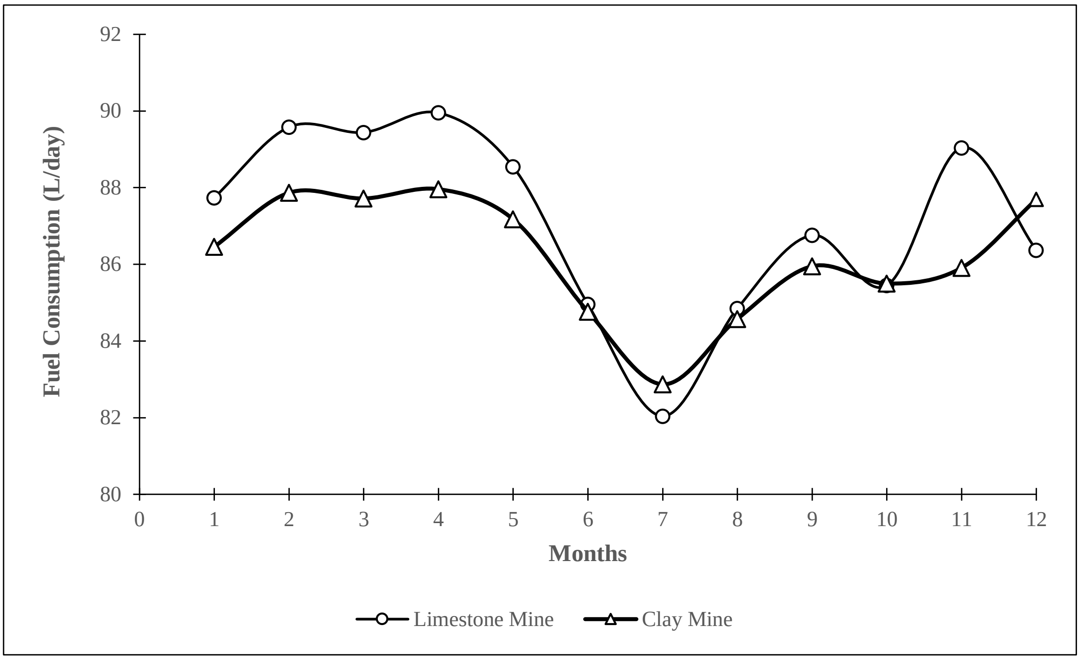

Figure 4.5. Average Daily Fuel Consumption for the Trucks of Limestone Mine (a) and of Clay Mine (b) by Month

The precipitation effect on truck fuel rate profiles was also evaluated according to sunny and rainy-day statistics, as shown in Table 4.6. Since the rolling resistance coefficient is an effective parameter in estimating fuel consumption and changes drastically in wet ground, a 15-25% variation is observed between the sunny and rainy days.

Table 4.6. *The Average Daily Fuel Consumption of Rainy and Sunny Days*

	Limestone Mine	**Clay Mine**
Sunny day	80 L/day	81 L/day
Rainy day	99 L/day	94 L/day

4.3.2 Effect of Payload

Trucks with the nominal and maximum payload capacities of 38.2 and 42 tonnes are operated in both the limestone and clay mines. The loading process in the model is activated in the excavator locations. Payload shows a variation in compliance with normal distribution, as discussed in Section 4.2. Therefore, fuel consumption rates are expected to differ in each cycle, accordingly. On this basis, the average amount of material hauled by a truck from the limestone mine to the plant is around 220 tonnes a day, and daily fuel consumption of 87 L is expected. Therefore, the fuel consumption in terms of L per tonne of hauled limestone is about 0.4 L/tonne. Figure 4.6 represents the correlation between daily fuel consumption and payload for the limestone mine trucks in January. The other months also exhibit similar behavior. R-squared value of 94.36% in the graph reveals the strong correlation between the payload and fuel consumption values. Any increase in the vehicle's gross weight will make a noticeable increase in the rimpull force requirement.

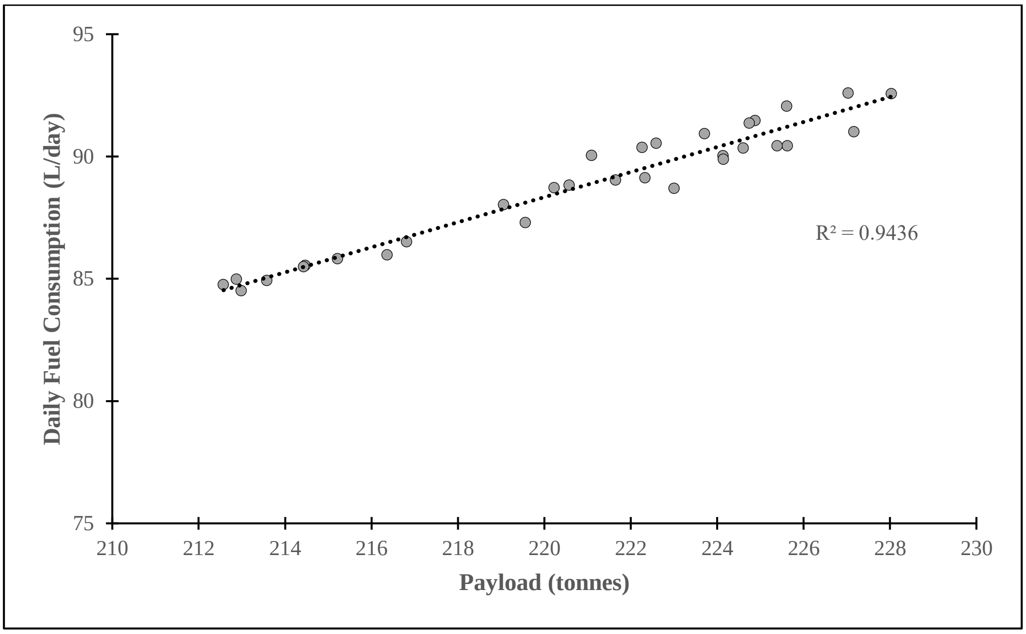

Figure 4.6. Correlation Between Daily Fuel Consumption and Payload

Distances to the plant, total daily productions, and truck numbers are different for both mines. Since the clay mine is closer to the plant and operated with fewer trucks, each truck needs to yield a higher daily production, around 380 tonnes. As discussed previously in Figure 4.5, the total amount of fuel consumed a day is similar for both mines. Therefore, the fuel consumption in terms of liters per tonne of hauled clay is around 0.23 L/tonne.

Table 4.7 shows the fuel rates in terms of liters per kilometer for the limestone and clay trucks' empty and loaded travels. The average fuel rate is calculated by dividing the route-based fuel consumption to the total route distance. Average fuel rates are 0.51 L/km and 0.46 L/km for the loaded and empty trucks operated in the limestone mine, respectively. On the other hand, these values are 0.72 L/km and 0.42 L/km for the clay mine's full and empty trucks, respectively. Both road and payload parameters are expected to be more effective in the travels of the clay mine trucks so that a 70% jump is observed between the fuel consumptions of the loaded and empty trips.

Table 4.7. *Fuel Rates of Loaded and Empty Trucks*

	Limestone Mine Trucks			**Clay Mine Trucks**		
	Fuel Consumption (L)	Route Distance (km)	Fuel Rate (L/km)	Fuel Consumption (L)	Route Distance (km)	Fuel Rate (L/km)
Loaded	8.11	16	0.51	5.45	7.58	0.72
Empty	7.36	16	0.46	3.21	7.58	0.42

The routes between the mine sites and the crushers have various road segments with different road characteristics. The road grades can be uphill, downhill, or flat. To better understand the payload effect, one of the flat road segments in the route between clay mine and crusher was chosen and analyzed (Figure 4.7). On rainy days, fuel rates of loaded and empty trucks are approximately 0.9 L/km and 0.4 L/km, while these values are 0.68 L/km and 0.33 L/km for sunny weathers, respectively.

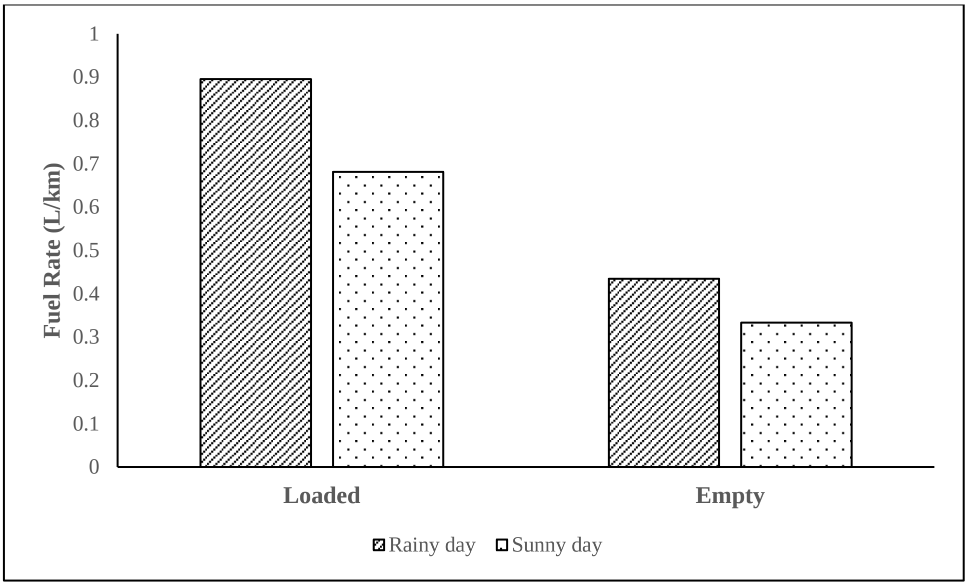

Figure 4.7. Fuel Rates for Loaded and Empty Trucks in Rainy and Sunny Days

4.3.3 Effects of Road Characteristics

Road characteristics, especially road grade and road surface properties, have a significant impact on fuel consumption. As the trucks move on road segments with different characteristics, the speed levels and amount of fuel consumed can differ dynamically. Speed and fuel consumption profiles through road segments with varied attributes on the routes between the locations that a truck can travel in a day are drawn to analyze the effect of road-related parameters.

Figure 4.8 illustrates how truck speed and fuel consumption values variate at the route from Excavator-1 in the limestone mine to Crusher1 (a) and its return path (b), depending on the road segment profiles and the precedence in the road intersections. As seen in the figure, road grade has an observable effect on fuel consumption rates. In uphill driving, fuel consumption rates are boosted since the truck engine needs to overcome a higher amount of resistive forces. On the other hand, fuel consumption rates drop to zero in the downhill direction. The vehicle is equipped with a deceleration fuel cut-off mechanism in a downhill direction, preventing fuel injection to the engine if it is in gear, not in gear idling condition. Besides, the fuel consumption rate is set to zero while braking either in uphill or downhill movement. Figure 4.8 (a) has many downhill road segments. Therefore, the fuel rate in these road segments drops to 0 L/h. The maximum fuel rate is observed at a distance between 10th and 12th km from the limestone mine. The highest observed fuel consumption rate is around 35 L/h. Figure 4.8 (b) shows that the effect of road garde on fuel rate becomes more observable at the return way segment that is 1 km away from the limestone mine. Once the segment grade turns to 8.9°, the fuel rate shows a sudden jump to 40 L/h, which is the maximum fuel rate of this route.

It is also observed from the figure that payload has a remarkable effect on fuel consumption. The fuel rate for loaded trucks is higher than the empty truck rate at the flat road segments. For example, at the last road segment of Figure 4.8 (a), a loaded truck consumes approximately 9 L/h. At the same road segment, which is the first road segment of Figure 4.8 (b), an empty truck consumes 5 L/h, which is nearly half of the loaded truck's fuel rate.

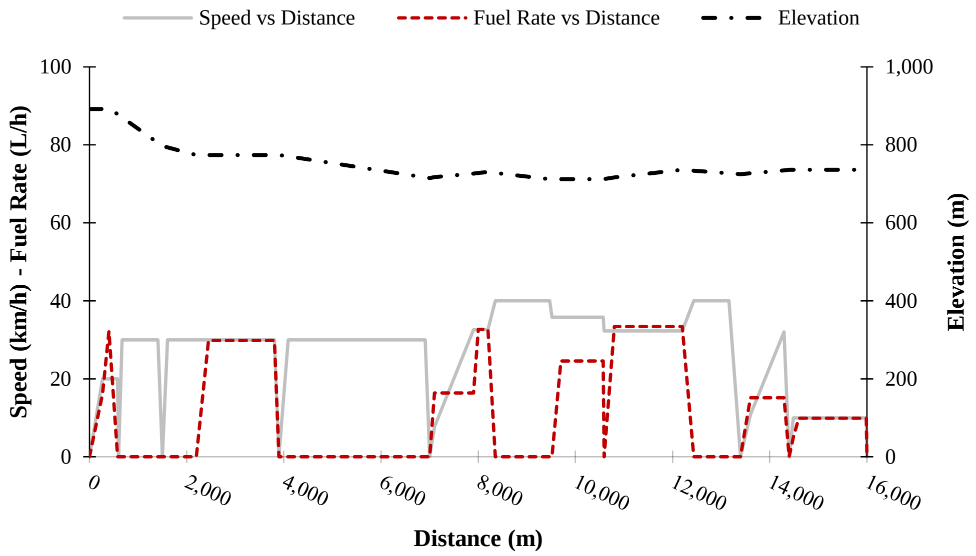

(a)

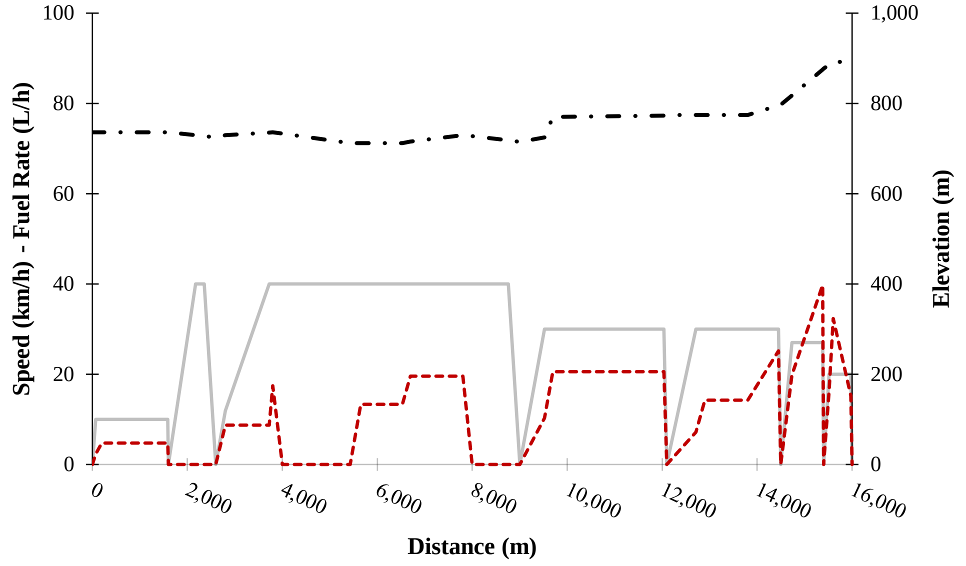

(b)

Figure 4.8. Vehicle Speeds and Fuel Consumption Rates in Time for the Route from the Limestone Mine Excavator1 to Crusher1 (a) and Its Return Path (b)

Figure 4.9 shows the speed, fuel rate, and elevation profiles for the route from the excavator in the clay mine to Crusher 2 (a) and its return route (b). The truck needs to stop at the intersection points; therefore, the speed and fuel rate drop to a minimum. As can be seen from the elevation profile of Figure 4.9 (a), the truck does not consume any fuel in a downhill direction where the fuel cut-off mechanism becomes active in cases where assistive forces overcome resistive forces, and the driver stops stepping on the gas. Correspondingly, the truck climbs to reach the clay mine in the last 1.5 km of the road shown in Figure 4.9 (b), so the fuel rate increases up to 31 L/h.

Considering the road grade and payload factors, the maximum fuel consumption rate can be seen on the road segment where a loaded truck is driven on the steepest road grade. For example, fuel consumption rates peaks at 45 L/h when located 3 km away from the clay mine under these conditions (Figure 4.9 (a)).

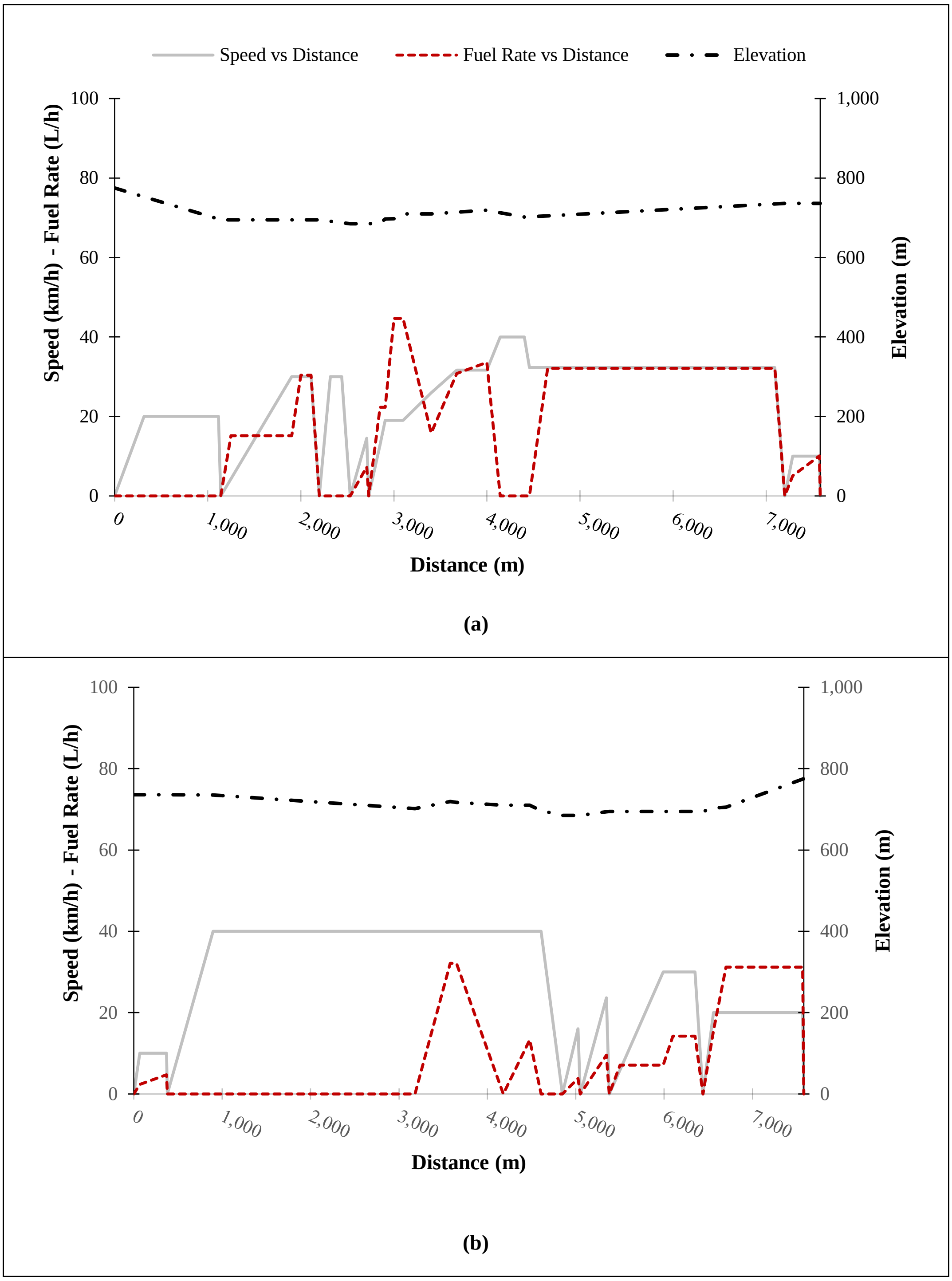

Figure 4.9. Vehicle Speeds and Fuel Consumption Rates in Time for the Route from the Clay Mine Excavator to Crusher2 (a) and Its Return Path (b)

According to the company's authorities, the average fuel consumption per 100 km is 50 L in summers and 55 L in winters. The developed model results show the fuel rate, including all trucks operated in both two mines, is 55.8 L/100 km on average in winter, rainy days, and 45 L/100 km in summer, sunny days. This slight difference can be due to the missing information about the truck maintenance records and truck deterioration levels that may affect the fuel consumption. Moreover, driver-related factors can also be effective in the fuel consumption behaviors of trucks. In brief, the company authorities validated the model's outcomes, considering the limitations.

4.3.4 Greenhouse Gas Emissions

Trucks emit greenhouse gases into the environment while consuming diesel fuel. To prevent harmful impacts on the environment, monitoring and controlling greenhouse gas (GHG) emissions is very important. GHG emissions and fuel consumption are related to each other, and one can be converted to another. This correlation is described in Equation 4.1 (Kecojevic and Komljenovic, 2010):

$$\mathrm{CO}_{2-\mathrm{e}} = \mathrm{FC} * \mathrm{EF} \tag{4.1}$$

Where FC is the fuel consumption in kL and EF is the emission factor. The emission factor for diesel haul trucks is 2.7 tonnes of $CO_{2\text{-}e}$ per kL of fuel (EPA, 2008). According to this calculation, a loaded truck operated in the limestone mine emits 22.03 kg of CO_2 and empty truck emits 19.87 kg of CO_2 on the route between the mine site and the crusher. Moreover, loaded and empty clay mine trucks emit 14.74 kg of CO_2 and 8.6 kg of CO_2, respectively. Daily fuel consumption rates of these types of trucks are almost same because of different total distances and number of cycles and around 216 kg of CO_2 are emitted by a single truck during a day.

The summary of the cycle results for both limestone and clay mine trucks are listed in Table 4.8. The truck number in the limestone mine is nearly three times the number of the trucks operated in the clay mine. In addition to that, the distance from the limestone mine to the crusher is almost twice the distance from the clay mine. For these reasons, the average cycle times of clay mine trucks are nearly half of the limestone mine trucks. Cycle time is the summation of the durations when the truck travels between loading and dumping points and includes loading, dumping, and waiting times. Traveling time from the clay mine to the crusher is around 23 minutes, and the return path's traveling time is 21 minutes. Additionally, the limestone mine trucks complete the route from the mine site to the crusher within around 42 minutes on average. It is observed that they also spend 42 minutes in the return path. Therefore, the total expected traveling times are 84 min and 44 min for limestone and clay mine trucks, respectively. There is a single fuel station so, the maximum queueing time occurs at this location. As for the payload, both types of trucks carry the same load amount in one cycle.

Table 4.8. *Cycle-related Output Data*

Elements	**Limestone Mine Trucks**	**Clay Mine Trucks**
Average number of cycle/day	5.85	9.90
Average cycle time	92 min	49 min
Average traveling time	84 min	44 min
Average queue time at crusher	4.22 min	1.45 min
Average queue time at fuel station	7.2 min	7.2 min
Average payload	39 tonnes	39.5 tonnes
Average GHG emissions	216 kg CO_2	216 kg CO_2

CHAPTER 5

CONCLUSION AND RECOMMENDATIONS

5.1 Conclusions

In surface mines, trucks are used for hauling ore and waste material between various destinations and account for the majority of operating costs. Among the cost items, fuel is the main contributor up to a percentile weight of 60 percent, depending on the truck configuration. On this basis, truck dispatching systems may cause an observable financial burden for mines. Besides, greenhouse gas emissions arising from fuel burning in engines lead to mining-induced environmental issues. At this point, any tactical, strategical, or operational improvement in a haulage system in terms of fuel consumption may provide a noticeable financial and energy saving. This research study intends to develop a simulation algorithm based on microscopic modeling to reveal the haul trucks' fuel consumption profiles in surface mines. The study methodology includes i) determination of the parameters that may have a moderate or strong dependency with a vehicle fuel consumption behavior, ii) development of a discrete-event simulation (DES) model considering micro-scale kinematic interactions between the operational environment and vehicles, iii) acquisition and processing of data to be used in a case study, iv) implementation of the DES model for the hauling operations of a cement company, and v) evaluation and analysis of the simulation outcomes.

In this sense, the current algorithm entails integrating various sub-models to estimate and correlate force, motion, and fuel consumption values to perform simultaneous monitoring. The developed algorithm is introduced into a discrete event simulation environment called Rockwell Arena Simulation. Periodic fuel consumption rates of individual trucks and truck fleets can be evaluated on a location and time basis. In addition, the effects of various factors such as speed, payload, weather, grade, and rolling resistance on fuel consumption and emissions are allowed to be analyzed comparatively.

The algorithm is then applied for a cement company where different routes between two separate mines, cement plant, and the other supportive activities are available in the operation area. At this point, two mines and a processing plant for the production of cement. Limestone and clay mines achieve a daily production of 4,500 tonnes and 1,200 tonnes and are located at 7.6 km and 16 km away from the plant, respectively. Trucks with a payload capacity of 40 tonnes are employed in the operations where fifteen different routes, which hold varying numbers of segments with different lengths, grades, and types, are actively used. Resistive and assistive forces effective on truck movement are estimated considering rolling resistances of road types, available speed limits, junction precedence in the active road network, and random precipitation probabilities in the region. Moreover, fuel consumption values during engine idling times in the loading, dumping, queuing, and refueling activities are also covered in the analysis where the activity durations are assigned randomly using the related data distributions.

Among the potential routes, the IDs labeled as 1 to 6 refer to the main routes between the excavators in the mines to the plant and needs a detailed fuel consumption analysis. The simulation monitoring data reveals that the average daily fuel consumed for the trucks operated in the limestone mine and the clay mine is 87 L. Their daily fuel consumption is almost the same. However, the amount of load that a truck carries during a day is different from each other. For this reason, the fuel rate is 0.4 L/tonne for limestone mine trucks, where it is 0.23 L/tonne for clay mine trucks. It is seen that payload is the primary determinant of the fuel consumption variation. Road grade is another factor effective in the consumption rate. At this point, it is observed that the fuel rate may show a sudden jump to 40 L/h for the segment grade of 8.9° while it is around 20L/h in the uphill direction along the route.

5.2 Recommendations

A comprehensive simulation model was constructed for time- and location-based evaluation of fuel consumption behaviors for individual vehicles and a joint operation of multiple vehicles. Following recommendations are provided for the improvement of the model in future studies:

i. In this research study, trucks are allowed to be interacted in the queues available in the loading, dumping, and refueling activities at the destinations of excavators, crushers, and fuel stations. The model can be improved more by interacting trucks each other during the movement.

ii. In future studies, drivers' influence on fuel consumption rates can be considered by evaluating and correlating the driving behavior model with the vehicle motion model. On this basis, the driver aggressiveness level of an operating mine can be characterized to measure the effects of human-based errors on fuel consumption and carbon emissions.

iii. Maintenance, machinery deterioration, and tire wear models can be included since they are expected to significantly affect the unit consumption rate per tonne of hauled material.

iv. Long-term production plans can be incorporated into the model, inducing a dynamic interaction of the force, motion, and fuel models according to the variations in pit geometry, haul road lengths/grades, and excavators' locations.

REFERENCES

Ahn, K. and Rakha, H. (2008). The effects of route choice decision on vehicle energy consumption and emissions. Transportation Research Part D: Transport and Environment. 13, 151-167.

Ahn, K., Rakha, H., Trani, A. and Aerde, M. (2002). Estimating Vehicle Fuel Consumption and Emissions Based on Instantaneous Speed and Acceleration Levels. Journal of Transportation Engineering, 129, 579-581.

Akcelik, R. (1985). An interpretation of the parameters in the simple average travel speed model of fuel consumption. Australian Road Research, 15, 46-49.

Akçelik, R. and Belsey, M. (2003). Operating cost, fuel consumption, and emission models in aaSIDRA and aaMOTION. 25th Conference of Australian Institutes of Transport Research.

An, F., Barth, M., Norbeck, J. and Ross, M. (1997). Development of comprehensive modal emission model: operating under hot-stabilized conditions. Transportation Research Record, Journal of the Transportation Research Board, National Academy of Sciences, 1587, 52-62.

Asadi, B. and Vahidi, A. (2010). Predictive Cruise Control: Utilizing Upcoming Traffic Signal Information for Improving Fuel Economy and Reducing Trip Time. IEEE Transactions on Control Systems Technology, 19, 3, 707-714.

Awuah-Offei, K., Osei, B. and Askari-Nasab, H. (2011). Modeling truck/shovel energy efficiency under uncertainty. Transactions of the Society for Mining, Metallurgy and Exploration, 330, 573-584.

Bajany, D., Zhang, L., and Xia, X. (2019). An Optimization Approach for Shovel Allocation to Minimize Fuel Consumption in Open-pit Mines: Case of Heterogeneous Fleet of Shovels. IFAC-PapersOnLine, 52(14), 207-212.

Banks, J., Carson, J. S., Nelson, B. L. and Nicol, D. M. (2010). Discrete-event system simulation. Fifth Edition.

Barlow, T. J. and Boulter, P. G. (2009). Emission factors 2009: Report 2 - a review of the average- speed approach for estimating hot exhaust emissions. Transport Research Laboratory Project Report.

Barlow, T. J., Hickman, A. J. and Boulter, P. G. (2001). Exhaust emission factors 2000: Database and emission factors. Transport Research Laboratory Project Report.

Barth, M. and Boriboonsomsin, K. (2008). Real-World Carbon Dioxide Impacts of Traffic Congestion. Transportation Research Record: Journal of the Transportation Research Board, 2058, 163-171.

Bektaş, T. and Laporte, G. (2011). The Pollution-Routing Problem. Transportation Research Part B.

Bigazzi, A. Y. and Bertini, R. L. (2009). Adding green performance metrics to a transportation data archive. Transportation Research Record, 2121, 30-40.

Bigazzi, A. Y. and Clifton, K. (2015). Modeling the Effects of Congestion on Fuel Economy for Advanced Power Train Vehicles. Civil and Environmental Engineering Faculty Publications and Presentations, 182.

Boriboonsomsin, K. and Barth, M. (2009). Impacts of road grade on fuel consumption and carbon dioxide emissions evidenced by use of advanced navigation systems. Transportation Research Record, 2139(1), 21-30.

Boriboonsomsin, K., Barth, M. J., Zhu, W. and Vu, A. (2012). Eco-Routing Navigation System Based on Multisource Historical and Real-Time Traffic Information. IEEE Transactions on Intelligent Transportation Systems, 13, 1694-1704.

Brundell-Freij, K. and Ericsson, E. (2005). Influence of street characteristics, driver category and car performance on urban driving patterns. Transportation Research Part D: Transport and Environment, 10, 3, 219-229.

Caterpillar. (2014). Caterpillar Performance Handbook. 44th Edition.

De Vlieger, I., De Keukeleere, D. and Kretzschmar, J. G. (2000). Environmental effects of driving behavior and congestion related to passenger cars. Atmospheric Environment, 34, 27, 4649-4655.

Demir, E., Bektaş, T. and Laporte, G. (2011). A comparative analysis of several vehicle emission models for road freight transportation. Transportation Research Part D: Transport and Environment, 16, 347-357.

Demir, E., Bektaş, T. and Laporte, G. (2012). An adaptive large neighborhood search heuristic for the pollution-routing problem. European Journal of Operational Research, 223(2), 346-359.

Demir, E., Bektaş, T. and Laporte, G. (2014). A review of recent research on green road freight transportation. European Journal of Operational Research, 237(3), 775-793.

EAPA _ Eurobitum. (2004). Environmental impacts and fuel efficiency of road pavements. Industry Report, March 2004.

Ejsmont, J., Sjögren, L., Swieczko-Zurek, B. and Ronowski, G. (2015). Influence of Road Wetness on Tire-Pavement Rolling Resistance. Journal of Civil Engineering and Architecture. 9.

Ericsson, E., Larsson, H. and Brundell-Freij, K. (2006). Optimizing route choice for lowest fuel consumption – Potential effects of a new driver support tool. Transportation Research Part C: Emerging Technologies, 14, 369-383.

Faris, W., Kafafy, R., Rakha, H. and Idres, M. (2011). Vehicle fuel consumption and emission modelling: An in-depth literature review. International Journal of Vehicle Systems Modelling and Testing, 6, 318-395.

Feng, Y., Fullerton, D. and Gan, L. (2005). Vehicle Choices, Miles Driven and Pollution Policies. Journal of Regulatory Economics, 44(1).

Ferrara, A., Sacone, S. and Siri, S. (2018). Emission Models for Freeway Traffic Systems. In Freeway Traffic Modelling and Control, 293-311.

Fonseca, N., Casanova, J. and Valdes, M. (2011). Influence of the stop/start system on CO_2 emissions of a diesel vehicle in urban traffic. Transportation Research Part D: Transport and Environment, 16, 194-200.

Fontaras, G., Zacharof, N. and Ciuffo, B. (2017). Fuel consumption and CO2 emissions from passenger cars in Europe Laboratory versus real-world emissions. Progress in Energy and Combustion Science, 60, 97-131.

Fu, J., and Bortolin, G. (2012). Gear Shift Optimization for Off-road Construction Vehciles. Procedia - Social and Behavioral Sciences, 54, 989-998.

Gallus, J., Kirchner, U., Vogt, R. and Benter, T. (2017). Impact of driving style and road grade on gaseous exhaust emissions of passenger vehicles measured by a Portable Emission Measurement System (PEMS). Transportation Research Part D: Transport and Environment, 52, 215-226.

Green, S. M., Ulm, A. and Gregory, F. J. (2013). Pavement roughness and fuel consumption. Concrete Sustainability Hub, MIT.

Greenwood, I. B. C. (2003). The effects of traffic congestion on fuel consumption.

Hockenos, P. and Wehrmann, B. (2018). Road freight emissions in Germany. Journalism for the energy transition. Retrieved from https://www.cleanenergywire.org/factsheets/road-freight-emissions-germany

Huang, Y., Ng, E. C. Y., Zhou, J. L., Surawaski, N. C., Chan, E. F. C. and Hong, G. (2018). Eco- driving technology for sustainable road transport: A review. Renewable and Sustainable Energy Reviews, 93, 596-609.

Iwata, Y., Otake, H. and Takagi, M. (2012). Results from Simulation Evaluation of Green Wave Advisory System. 19^{th} ITS World Congress, Austria.

Javanmardi, S., Bideaux, E., Trégouët, J. F., Trigui, R., Tattegrain, H. and Bourles, En. N. (2017). Driving Style Modelling for Eco-driving Applications. IFAC PapersOnLine, 50, 1, 13866-13871.

Kaufman, W. W. and Ault. J. C. (1977). Design of surface mine haulage roads. A Manual.

Kecojevic, V. and Komljenovic. D. (2010). Haul truck fuel consumption and CO_2 emission under various engine load conditions. Mining Engineering, 62, 44-48.

Kelton, W. D., Sadowski, R. P. and Sadowski, D. A. (2004). Simulation with Arena Second Edition.

Khader, A. I. and Martin, R. S. (2019). On-the-road testing of the effects of driver's experience, gender, speed and road grade on car emissions. Journal of Air & Waste Management Association, 69, 10, 1182-1194.

Li, W., Wu, G., Zhang, Y. and Barth, M. J. (2017). A comparative study on data segregation for mesoscopic energy modeling. Transportation Research Part D: Transport and Environment, 50, 70-82.

Ligterink, N., Smokers, R. T., Spreen, J., Mock, P. and Tietge, U. (2016). Supporting analysis on real-world light-duty vehicle CO2 emissions. Delft, the Netherlands: TNO.

Liu, X. (2015). A more accurate method using MOVES (Motor Vehicle Emission Simulator) to estimate emission burden for regional-level analysis. Journal of the Air & Waste Management Association, 65, 7, 837-843.

Masikos, M., Demestichas, K., Adamopoulou, E. and Theologou, M. (2015). Energy efficient routing based on vehicular consumption predictions of a mesoscopic learning model. Applied Soft Computing. 28, 114-124.

Meseguer, J. E., Toh, C. K., Calafate, C. T., Cano, J. C. and Manzoni, P. (2017). Drivingstyles A mobile platform for driving styles and fuel consumption characterization. Journal of Communications and Networks, 19, 2, 162-168.

Mickünaitis, V., Pikünas, A. and Mackoit, I. (2007). Reducing fuel consumption and CO2 emission in motor cars. Transport, 22, 160-163.

Morse, S. (2018). Analysis the use of sustainability indicators. The Palgrave Handbook of Indicators in Global Governance.

Park, S. and Rakha, H. (2006). Energy and Environmental Impacts of Roadway Grades. Transportation Research Record, 1987(1), 148-160.

Parreira, J. (2013). An Interactive Simulation Model to Compare an Autonomous Haulage Truck System with a Manually-Operated System.

Parreira, J. and Meech, J. (2011). Autonomous Haulage Systems – Justification and Opportunity. Autonomous and Intelligent Systems, International Conference IS2011.

Pekula, N., Kuritz, B., Hearne, J., Marchese, A., and Hesketh, R. (2003). The Effect of Ambient Temperature, Humidity, and Engine Speed on Idling Emissions from Heavy-Duty Diesel Trucks. SAE Transactions, 112, 148-158.

Plotkin, S. and Ribeiro, S. K. (2009). Energy efficiency technologies for road vehicles. Energy Efficiency, 2, 125-137.

Rodovalho, E. D., Lima, H. M., and Tomi, G. D. (2016). New approach for reduction of diesel consumption by comparing different mining haulage configurations. Journal of Environmental Management, 172, 177-185.

Rodrigue, J. P. (2020). Transport, Energy and Environment. In The Geography of Transport Systems.

Saboohi, Y., and Farzaneh, H. (2009). Model for developing an eco-driving strategy of a passenger vehicle based on the least fuel consumption. Applied Energy, 86, 1925-1932

Sahoo, L. K., Bandyopadhyay, S., and Banerjee, R. (2014). Benchmarking energy consumption for dump trucks in mines. Applied Energy, 113, 1382-1396.

Scora, G. and Barth, M. (2006). Comprehensive Modal Emissions Model (CMEM) User's Guide.

Siami-Irdemoosa, E., and Dindarloo, S. R. (2015). Prediction of fuel consumption of mining dump trucks: A neural networks approach. Applied Energy, 151, 77-84.

Sivak, M. and Schoettle, B. (2012). Eco-driving: Strategic, tactical and operational decisions of the driver that influence vehicle fuel economy. Transport Policy, 22, 96-99.

Soofastaei, A., Aminossadati, S. M., Kizil, M. S. and Knights, P. (2016). Reducing Fuel Consumption of Haul Trucks in Surface Mines Using Artificial Intelligence Models. Proceedings of the 16th Coal Operators' Conference, 477-489.

Tatiya, R. (2012). Surface and Underground Excavations: Methods, Techniques and Equipment. CRC Press.

Tielert, T., Killat, M., Hartenstein, H., Luz, R., Hausberger, S. and Benz, T. (2010). The impact of traffic-light-to-vehicle communication on fuel consumption and emissions. Internet of Things (IOT), 1-8.

Tolouei, R., and Titheridge, H. (2009). Vehicle mass as a determinant of fuel consumption and secondary safety performance. Transportation Research Part D: Transport and Environment, 14, 385-399.

United States Environmental Protection Agency (EPA). (2016). Description and History of the MOBILE Highway Vehicle Emission Factor Model. Retrieved from https://www.epa.gov/moves/description-and-history-mobile-highway-vehicle-emission-factor-model

United States Environmental Protection Agency (EPA). (2019). The 2019 EPA Automotive Trends Report: Greenhouse Gas Emissions, Fuel Economy and Technology since 1975 – Executive Summary. Retrieved from https://www.epa.gov/sites/production/files/2020-03/documents/420s20001.pdf.

U.S. Energy Information Administration (EIA). (2019). Use of energy. Retrieved from https://www.eia.gov/energyexplained/use-of-energy/

Walsh, M. P. (2003). Vehicle emissions and health in developing countries. In Air Pollution and Health in Rapidly Developing Countries, 146-176.

Yao, Y., Zhao, X., Zhang, Y., Chen, C. and Rong, J. (2020). Modeling of individual vehicle safety and fuel consumption under comprehensive external conditions. Transportation Research Part D: Transport and Environment, 79.

Yue, H. (2008). Mesoscopic fuel consumption and emission modelling. Doctor of Philosophy dissertation, Virginia Polytechnic Institute and State University.

Yue, H. and Rakha, H. (2008). Validation of the VT-Meso vehicle fuel consumption and emission model. In Efficient Transportation and Pavement Systems: Characterization, Mechanisms, Simulation and Modeling, 97-114.

Zacharof, N., Fontaras, G., Ciuffo, B., Tsiakmakis, S., Anagnostopoulos, K., Marotta, A. and Pavlovic, J. (2016). Review of in use factors affecting the fuel consumption and CO2 emissions of passenger cars.

Zhou, M., Jin, H., and Wang, W. (2016). A review of vehicle fuel consumption models to evaluate eco-driving and eco-routing. Transportation Research Part D: Transport and Environment, 49, 203-218.

APPENDICES

A. Road Segment Data Set

Table A.1. Road Segment Data for Routes ID 1 and 2

Segment ID	Length (km)	Road Grade	Road Type	Inter section	Segment ID	Length (km)	Road Grade	Road Type	Inter section
$S_{1,1}$	0.40	0.00°	3	0	$S_{2,1}$	0.40	0.00°	3	0
$S_{1,2}$	0.20	-7.50°	3	1	$S_{2,2}$	0.20	-7.50°	3	1
$S_{1,3}$	0.90	- 8.89°	2	1	$S_{2,3}$	0.90	- 8.89°	2	1
$S_{1,4}$	0.70	- 3.29°	2	0	$S_{2,4}$	0.70	- 3.29°	2	0
$S_{1,5}$	1.70	0.00°	2	1	$S_{2,5}$	1.70	0.00°	2	1
$S_{1,6}$	3.10	- 1.90°	2	1	$S_{2,6}$	3.10	- 1.90°	2	1
$S_{1,7}$	1.20	1.33°	1	0	$S_{2,7}$	1.20	1.33°	1	0
$S_{1,8}$	1.27	- 1.40°	1	0	$S_{2,8}$	1.27	- 1.40°	1	0
$S_{1,9}$	1.10	0.00°	1	0	$S_{2,9}$	1.10	0.00°	1	0
$S_{1,10}$	1.63	1.47°	1	0	$S_{2,10}$	1.63	1.47°	1	0
$S_{1,11}$	1.20	- 0.93°	1	1	$S_{2,11}$	1.20	- 0.93°	1	1
$S_{1,12}$	1.00	1.10°	1	1	$S_{2,12}$	1.00	1.10°	1	1
$S_{1,13}$	1.60	0.00°	4	2	$S_{2,13}$	1.60	0.00°	4	2

Table A.2. Road Segment Data for Routes ID 4 and 5

Segment ID	Length (km)	Road Grade	Road Type	Inter section	Segment ID	Length (km)	Road Grade	Road Type	Inter section
$S_{4,1}$	0.63	0.00°	4	1	$S_{5,1}$	0.10	2.00°	4	0
$S_{4,2}$	0.344	- 2.32°	1	2	$S_{5,2}$	0.202	0.00°	4	0
					$S_{5,3}$	0.124	- 2.43°	4	1
					$S_{5,4}$	0.194	- 2.06°	4	2

Table A.3. Road Segment Data for Routes ID 6 and 7

Segment ID	Length (km)	Road Grade	Road Type	Inter section	Segment ID	Length (km)	Road Grade	Road Type	Inter section
$S_{6,1}$	1.60	0.00°	4	1	$S_{7,1}$	1.60	0.00°	4	1
$S_{6,2}$	1.00	- 1.10°	1	1	$S_{7,2}$	1.00	- 1.10°	1	1
$S_{6,3}$	1.20	0.93°	1	0	$S_{7,3}$	1.20	0.93°	1	0
$S_{6,4}$	1.63	- 1.47°	1	0	$S_{7,4}$	1.63	- 1.47°	1	0
$S_{6,5}$	1.10	0.00°	1	0	$S_{7,5}$	1.10	0.00°	1	0
$S_{6,6}$	1.27	1.41°	1	0	$S_{7,6}$	1.27	1.41°	1	0
$S_{6,7}$	1.20	- 1.33°	1	1	$S_{7,7}$	1.20	- 1.33°	1	1
$S_{6,8}$	3.10	1.90°	2	1	$S_{7,8}$	3.10	1.90°	2	1
$S_{6,9}$	1.70	0.00°	2	0	$S_{7,9}$	1.70	0.00°	2	0
$S_{6,10}$	0.70	3.28°	2	1	$S_{7,10}$	0.70	3.28°	2	1
$S_{6,11}$	0.90	8.89°	2	1	$S_{7,11}$	0.65	0.00°	2	1
$S_{6,12}$	0.20	7.5°	3	0	$S_{7,12}$	0.60	6.50°	3	0
$S_{6,13}$	0.40	0.00°	3	2	$S_{7,13}$	0.20	- 7.00°	3	2

Table A.4. Road Segment Data for Routes ID 8 and 9

Segment ID	Length (km)	Road Grade	Road Type	Inter section	Segment ID	Length (km)	Road Grade	Road Type	Inter section
$S_{8,1}$	0.38	0.00°	4	1	$S_{9,1}$	0.37	2.43°	4	0
$S_{8,2}$	2.80	- 1.22°	1	0	$S_{9,2}$	1.00	0.00°	1	1
$S_{8,3}$	0.40	4.24°	1	0	$S_{9,3}$	1.00	- 1.10°	1	1
$S_{8,4}$	0.60	- 1.5°	1	0	$S_{9,4}$	1.20	0.93°	1	0
$S_{8,5}$	0.30	0.00°	1	0	$S_{9,5}$	1.63	- 1.47°	1	0
$S_{8,6}$	0.37	- 6.75°	1	1	$S_{9,6}$	1.10	0.00°	1	0
$S_{8,7}$	0.20	0.00°	2	1	$S_{9,7}$	1.27	1.41°	1	0
$S_{8,8}$	0.33	3.00°	2	1	$S_{9,8}$	1.20	- 1.33°	1	1
$S_{8,9}$	1.06	0.00°	2	1	$S_{9,9}$	3.10	1.90°	2	1
$S_{8,10}$	1.14	7.00°	3	2	$S_{9,10}$	1.70	0.00°	2	0
					$S_{9,11}$	0.70	3.28°	2	1
					$S_{9,12}$	0.90	8.89°	2	1
					$S_{9,13}$	0.20	7.50°	3	0
					$S_{9,14}$	0.40	0.00°	3	2

Table A.5. Road Segment Data for Routes ID 10 and 11

Segment ID	Length (km)	Road Grade	Road Type	Inter section	Segment ID	Length (km)	Road Grade	Road Type	Inter section
$S_{10,1}$	0.37	2.43°	4	0	$S_{11,1}$	2.21	- 1.22°	4	1
$S_{10,2}$	1.00	0.00°	1	1	$S_{11,2}$	0.40	4.24°	1	0
$S_{10,3}$	1.00	- 1.10°	1	1	$S_{11,3}$	0.60	- 1.50°	1	0
$S_{10,4}$	1.20	0.92°	1	0	$S_{11,4}$	0.30	0.00°	1	0
$S_{10,5}$	1.63	- 1.47°	1	0	$S_{11,5}$	0.37	- 6.75°	1	1
$S_{10,6}$	1.10	0.00°	1	0	$S_{11,6}$	0.20	0.00°	1	1
$S_{10,7}$	1.27	1.41°	1	0	$S_{11,7}$	0.33	3.00°	2	1
$S_{10,8}$	1.20	- 1.33°	1	1	$S_{11,8}$	1.06	0.00°	2	1
$S_{10,9}$	3.10	1.90°	2	1	$S_{11,9}$	1.14	7.00°	3	2
$S_{10,10}$	1.70	0.00°	2	0					
$S_{10,11}$	0.70	3.28°	2	1					
$S_{10,12}$	0.65	0.00°	2	1					
$S_{10,13}$	0.60	6.50°	3	0					
$S_{10,14}$	0.20	- 7.00°	3	2					

Table A.6. Road Segment Data for Routes ID 12 and 13

Segment ID	Length (km)	Road Grade	Road Type	Inter section	Segment ID	Length (km)	Road Grade	Road Type	Inter section
$S_{12,1}$	0.31	2.57°	4	1	$S_{13,1}$	0.12	- 2.50°	4	1
$S_{12,2}$	0.19	0.00°	4	1	$S_{13,2}$	1.12	0.00°	1	1
$S_{12,3}$	0.11	2.72°	1	2	$S_{13,3}$	1.00	- 1.10°	1	1
					$S_{13,4}$	1.20	0.92°	1	0
					$S_{13,5}$	1.63	- 1.47°	1	0
					$S_{13,6}$	1.10	0.00°	1	0
					$S_{13,7}$	1.27	1.40°	1	0
					$S_{13,8}$	1.20	- 1.33°	1	1
					$S_{13,9}$	3.10	1.90°	2	1
					$S_{13,10}$	1.70	0.00°	2	0
					$S_{13,11}$	0.70	3.28°	2	1
					$S_{13,12}$	0.90	8.89°	2	1
					$S_{13,13}$	0.20	7.50°	3	0
					$S_{13,14}$	0.40	0.00°	3	2

Table A.7. *Road Segment Data for Routes ID 14 and 15*

Segment ID	Length (km)	Road Grade	Road Type	Inter section	Segment ID	Length (km)	Road Grade	Road Type	Inter section
$S_{14,1}$	0.12	- 2.50°	4	1	$S_{15,1}$	2.35	- 1.10°	4	1
$S_{14,2}$	1.12	0.00°	1	1	$S_{15,2}$	0.52	-1.92°	1	1
$S_{14,3}$	1.00	- 1.10°	1	1	$S_{15,3}$	0.46	3.91°	1	0
$S_{14,4}$	1.20	0.92°	1	0	$S_{15,4}$	0.31	0.00°	1	0
$S_{14,5}$	1.63	- 1.47°	1	1	$S_{15,5}$	0.32	- 2.81°	1	0
$S_{14,6}$	1.10	0.00°	1	1	$S_{15,6}$	0.24	0.00°	2	0
$S_{14,7}$	1.27	1.40°	1	0	$S_{15,7}$	0.37	- 7.03°	2	1
$S_{14,8}$	1.20	- 1.33°	1	0	$S_{15,8}$	0.24	0.00°	2	1
$S_{14,9}$	3.10	1.90°	2	0	$S_{15,9}$	0.33	4.23°	2	1
$S_{14,10}$	1.70	0.00°	2	0	$S_{15,10}$	1.06	0.00°	3	1
$S_{14,11}$	0.70	3.28°	2	1	$S_{15,11}$	1.14	7.54°	3	2
$S_{14,12}$	0.65	0.00°	2	1					
$S_{14,13}$	0.60	6.50°	3	0					
$S_{14,14}$	0.20	- 7.00°	3	2					